Australian Government
Department of Defence
Defence Science and
Technology Organisation

DSTO

Modelling of PBX-115 Using Kinetic CHEETAH and the DYNA Codes

Jing Ping Lu and
David L. Kennedy

DSTO-TR-1496

20040412 028

Australian Government
Department of Defence
Defence Science and
Technology Organisation

Modelling of PBXW-115 Using Kinetic CHEETAH and the DYNA Codes

Jing Ping Lu and David L. Kennedy***

*** Weapons Systems Division**
Systems Sciences Laboratory

**** Orica Explosives**

DSTO-TR-1496

ABSTRACT

PBXW-115, a highly non-ideal explosive tailored for underwater effects and composed of 43% ammonium perchlorate, 25 % aluminium, 20% RDX and 12% HTPB binder, has been studied using Kinetic CHEETAH (the Lawrence Livermore National Laboratory CHEETAH 2.0 code), the three-term "Ignition and Growth" Model incorporated into the explicit finite element hydrocode LSTC-DYNA, and the CPeX Reactive Model based on the small divergent detonation theory of Wood and Kirkwood in DYNA2D. This report firstly focuses on a series of simulations performed using Kinetic CHEETAH based on the Wood-Kirkwood detonation theory using a pressure exponent of 2 in the pressure-dependent rate law. It was found that CHEETAH could predict the trend of the detonation velocity as a function of charge diameter, but overestimated the detonation velocities. The agreement was improved with further parameter adjustment, by decreasing the pressure exponent in the rate law from 2.0 to 1.0, and then 0.5. The reaction zone widths over a wide range of charge radius were also computed. Attention was then turned to hydrocode modelling, with particular interest in developing reactive models for PBXN-111 and PBXW-115 (*Aust*). Both the "Ignition and Growth" Model and the CPeX Model were calibrated against the experimentally observed dependence of detonation velocity on charge diameter in unconfined charges of both PBXW-115 (*Aust*) and US PBXN-111. These two reactive models were validated by comparing their predictions against experimental data for detonation of charges confined in 2.5 mm and 3 mm thick brass. The Ignition and Growth Model was then applied successfully to the simulation of aquarium tests. Finally, to test whether the two models using parameters derived from small-scale tests can be applied to large-scale devices, these two models were applied to the simulation of mid-scale underwater tests of PBXW-115 (*Aust*), and comparisons with available data are made. The LS-DYNA simulations of shock front curvature for unconfined charges are also presented and the relationships between the radii of curvature for the detonation fronts and self-propagating detonation velocities are discussed.

RELEASE LIMITATION

Approved for public release

Published by

DSTO Systems Sciences Laboratory
PO Box 1500
Edinburgh South Australia 5111 Australia

Telephone: (08) 8259 5555
Fax: (08) 8259 6567

AR-012-899
September 2003

APPROVED FOR PUBLIC RELEASE

Modelling of PBXW-115 Using Kinetic CHEETAH and the DYNA Codes

Executive Summary

In the energetic materials field, purely relying on experimental tests and trials to evaluate the performance and to understand the behaviour of new explosive compositions is no longer an efficient approach, because they are usually very costly, and often unpractical or even impossible for complex configurations. Therefore, there is a continuing need for a reliable numerical modelling technique as an alternative tool. PBXW-115, a extremely non-ideal explosive tailored for underwater effects and composed of 43% ammonium perchlorate, 25 % aluminium, 20% RDX and 12% HTPB binder, is a challenging explosive to model.

This report firstly focuses on a series of simulations performed using Kinetic CHEETAH based on the Wood-Kirkwood detonation theory using a pressure exponent of 2 in the pressure-dependent rate law. It was found that CHEETAH could predict the trend of the detonation velocity as a function of charge diameter, but overestimated the detonation velocities. The agreement was improved with further parameter adjustment, by decreasing the pressure exponent in the rate law from 2.0 to 1.0, and then 0.5. The reaction zone widths over a wide range of charge radius were also computed. Preliminary results using Kinetic CHEETAH indicate that the detonation velocity and the critical diameter are sensitive to the assumed AP decomposition rate. This might suggest that the observed differences between the US and the Australian composition are due to the particle size of the AP rather than the RDX. Further investigation of the effects of the assumed AP decomposition rate on the detonation velocity as a function of charge diameter will be carried out in the future.

Attention was then turned to hydrocode modelling, with particular interest in developing reactive models for PBXN-111 and PBXW-115 (*Aust*). Both the "Ignition and Growth" Model and the CPeX Model, although determined from the detonation velocity versus diameter effect experimental data for unconfined charges, could faithfully model the reaction rate characteristics for experiments carried out in other configurations. This was validated by comparing the predictions using both models against experimental data for detonation of charges confined in 2.5 mm and 3 mm thick brass. The Ignition and Growth Model was then applied successfully to the simulation of aquarium tests. Finally, to test whether the two models using parameters derived from small-scale tests can be applied to large-scale devices, these two models were applied to the simulation of mid-scale underwater tests PBXW-115 (*Aust*), and comparisons with available data were made. The LS-DYNA simulations of shock front curvature for unconfined charges are presented and the relationships between the radii of curvature for the detonation fronts and self-propagating detonation velocities of PBXN-111 are discussed. Given that there is a lack of experimental wave curvature data for PBXW-115(*Aust*), the simulation results presented herein provide some insight into the detonation process for this version of the explosive composition.

Authors

Jing Ping Lu
Weapons Systems Division

Jing Ping Lu was awarded a PhD in Civil Engineering at University of Wollongong in 1991. Before joining the Explosive Group, WSD at DSTO in March 2000, she was a senior research scientist in the Division of Building, Construction and Engineering, CSIRO where she spent 10 years working on modelling aspects of projects related to the structural use of different materials. She is currently conducting research into the performance prediction of explosive materials and the mathematical modelling and computer simulation of explosive behaviour.

David L. Kennedy
Orica Explosives
George Booth Drive
PO Box 196
Kurri Kurri, NSW 2327
On contract to Weapons Systems Division

Dr David Kennedy has 23 years experience as a research scientist with Orica (formerly ICI) Explosives, including a four month secondment to Los Alamos National Laboratory as a visiting scientist. His areas of theoretical research include reactive equations of state, mixing rules under detonation conditions, reaction rate laws for non-ideal explosives, and the dynamic fracture of brittle materials. His areas of applied research include the design of initiation systems, the investigation of blasting systems and techniques, the analysis and mitigation of explosive hazards, and the design and proofing of blast resistant structures.

Contents

1. Introduction

Since the development of PBXW-115* (43/25/20/12 AP/Al/RDX/HTPB), now known as PBXN-111* in the US after being fully qualified as an underwater explosive and accepted for a possible Insensitive Munition (IM) warhead fill by the US Navy [Anderson and Leahy 1985], research and development have been extensively conducted by many researchers for more than a decade.

- Forbes and co-workers at NSWC [Forbes et al. 1989; Forbes et al. 1992] have applied different experimental techniques to obtain detonation velocity and critical diameter for both unconfined and confined charges, corner turning ability and shock front curvature. This has provided a substantial data base on detonation properties of this non-ideal explosive, which can be used to calibrate hydrodynamic flow detonation models taking into account ignition and growth of reaction and multiple energy release rates.
- The CPeX model (Commercial Performance of Explosives) developed by Kirby and Leiper [1985] was applied by Jones and Kennedy [1991] to predict the properties of unconfined PBXW-115 and found excellent fit to the experimental data. The authors also made recommendations for future work including confinement and aquarium test modelling. The same CPeX model was implemented in the explicit finite element hydrocode DYNA2D to simulate time-dependent reactive flow in non-ideal explosives such as PBXN-111 for a variety of initiation and detonation tests [Kennedy and Jones 1993], with the results generally in excellent agreement with the experimental data.
- Miller [1996a] developed a simplified ignition and growth (SIG) model consisting of only two adjustable parameters, the ignition (I) and growth (G) rate constants determined by iterating these variables in DYNA2D hydrocode simulations of the failure diameter and the gap test sensitivity until the experimental values were reproduced. According to the author, there is a need to investigate how the pressure effects on reaction front radius of curvature and /or the reaction zone thickness can be used in further characterizing the chemical reaction rate kinetics of detonation. He and his co-worker [Miller 1996b; Miller and Guirguis 1996] also reported a reactive flow model developed for detonation and combustion processes for non-ideal metallised explosives that they implemented in DYNA2D. The model was based on a coupling of the global kinetics for the fast reactions that determine the detonation state and the slow metal combustion kinetics that determine the late time energy release after the CJ state.

* The terms PBXW-115 and PBXN-111 are used interchangeably. PBXW-115 was the name used before US Navy qualification. PBXN-111 is the name used post-qualification. PBXW-115(*Aust*) is the term used to identify the composition developed from indigenous Australian ingredients.

- For a number of explosives including PBXN-111, Souers [1997] developed a model to relate the size effects of a cylinder with its average sonic reaction zone length. This model assumed an external layer along the edge of the cylinder out of which all energy was considered lost. Two major size effects were identified, namely the "forward" effect (the reduction of the detonation velocity with the decrease of the radius until detonation finally stops) and the "transverse" effect (the increase of curvature of the detonation front with decreasing radius). The rate constants for time-dependent modelling were then estimated from reaction zone lengths based on either the detonation front curvature or charge diameter effects [Souers and Garza 1998].
- Souers [1998] also published a collection of detonation front curvature and size effect data, plus the calculated parameters that constitute the input to Kinetic CHEETAH. Howard et al. [1998] applied the renormalised new product library NEWC1 including a three-phase carbon equation of state (EOS) with the more reliable Murnaghan EOS for solids in CHEETAH to PBXN-111 prediction and achieved good agreement with experimental results.
- More recently, Souers et al [2001] have fully described and analysed the cylinder test for deriving detonation energies, including the relation between streak camera and Fabry-Perot interferometer data. They introduced CHEETAH 3.0 with its new all-Hugoniot calibration producing the most accurate detonation energies to date. Taking the composite explosive PBXN-111 as a special problem, they found that the Reactive Flow code JWL++ with one fully reacted JWL EOS failed to fit the data. By constructing a 2-JWL form with the first, fast rate describing the detonation velocity and the second, slow rate the cylinder energies, they have successfully applied the JWL++ to the non-ideal explosive PBXN-111 that reacts as little as 25% in the cylinder test.

An "Australianised" version of the US Navy IM underwater explosive PBXN-111, based on indigenous ingredients, was developed and designated PBXW-115 (*Aust*) [Bocksteiner and Billon 1991; Bocksteiner et al. 1994]. Research by Bocksteiner and Whelan first addressed binder and formulation studies, compatibility and sensitiveness, then detonation properties including velocity of detonation, critical diameter, shock sensitivity and finally underwater explosive performance [Bocksteiner and Billon 1991; Bocksteiner and Whelan 1994; Bocksteiner 1996]. They found that PBXW-115 (*Aust*) had significantly different explosive properties, particularly critical diameter and shock sensitivity, from its US counterpart, believed due to the particle size distribution, grade and type of RDX used in the two formulations. These investigations resulted in PBXW-115 (*Aust*) being qualified by Australian Ordnance Council for use as an insensitive main charge fill in large underwater blast weapons, and the proposal that the material could be qualified as an Extremely Insensitive Detonating Substance [Whelan and Bocksteiner 1998].

Turning attention to the modelling of the Australian version of PBXW-115, i.e. PBXW-115 (*Aust*), the limited work reported so far [Jones and Kennedy 1991] is confined only to modelling detonation velocity of unconfined PBXW-115 (*Aust*) where the model was

based on the results of experiments on relatively small charges. In order to validate extrapolation based on the experimental results on smaller charges to the larger explosive charges used in underwater devices, the Weapons Systems Division at DSTO-Edinbugh has been undertaking investigations into both modelling of realistic charge geometries and small scale to mid-scale underwater tests to record the "early-time" behaviour and performance of PBXW-115 (*Aust*). The results of the small-scale aquarium tests presented by Dorsett and Katselis [1999] and the mid-scale underwater tests reported by Wilkinson [2001] are two of the experimental investigations carried out, which can be used for calibrating computer models. A parallel modelling program was initially focussed on performance predictions with Lawrence Livermore National Laboratory CHEETAH 2.0 code based on both the traditional Chapman-Jouget (CJ) thermodynamic detonation theory and the Wood-Kirkwood kinetic detonation theory [Lu 2001].

Following the earlier studies of non-ideal explosive PBXW-115 performance [Lu 2001; Lu and Kennedy 2001], and in order to further characterize the non-ideal features of this explosive, this report firstly focused on a series of simulations performed using Kinetic CHEETAH based on the Wood-Kirkwood detonation theory using a pressure exponent of 2 in the pressure-dependent rate law. It was found that CHEETAH could predict the trend of the detonation velocity as a function of charge diameter, but overestimated the detonation velocities. The agreement was improved with further parameter adjustment by decreasing the pressure exponent in the rate law from 2.0 to 1 and then 0.5. The reaction zone widths over a wide range of charge radius were also computed.

Attention was then turned to hydrocode modelling, with particular interest in developing reactive models for PBXN-111 and PBXW-115 (*Aust*) [Lu et al 2002]. In this report, both the three-term "Ignition and Growth" Model incorporated into the explicit finite element hydrocode LS-DYNA, and the CPeX Reactive Model based on the small divergent detonation theory of Wood and Kirkwood in DYNA2D, have been calibrated against the experimentally observed dependence of detonation velocity on charge diameter in unconfined charges of both PBXW-115 (*Aust*) and US PBXN-111. These two reactive models were validated by comparing their predictions with experimental data for detonation of charges confined in 2.5 mm and 3 mm thick brass. The Ignition and Growth Model was then applied successfully to simulation of aquarium tests. Finally, to test whether the two models using parameters derived from small-scale tests can be applied to large-scale devices, these two models were applied to the simulation of mid-scale underwater tests on PBXW-115 (*Aust*), and comparisons with available data were made. The LS-DYNA simulations of shock front curvature for unconfined charges have also been presented and the relationship between the radii of curvature for the detonation fronts and self-propagating detonation velocities has been discussed.

2. Kinetic Calculations

Kinetic CHEETAH is based on the Wood-Kirkwood (WK) detonation theory [Wood and Kirkwood 1954] which is specially designed for modelling time-dependent phenomenon. The new chemical kinetics model implemented in CHEETAH considers detonation in composite explosives with large reaction zones, and the interplay between the energy produced by kinetically controlled reactions and the energy lost due to radial expansion of the product gases. Wood-Kirkwood theory thus allows prediction of the dependence of detonation parameters on charge diameters, and estimation of the length of the detonation zone, identified as the region behind the detonation wave for which the sum of the mass velocity and the velocity of sound is equal to the detonation velocity [Loboiko and Lubyatinsky 2000].

As described in the CHEETAH 2.0 User's Manual [Fried et al 1998], WK theory starts with the hydrodynamic Euler equations coupled to chemical kinetics. The theory treats the detonation along the centre of the cylinder. Radial expansion is treated as a first order perturbation to perfect one dimensional planar detonation. The Euler equations are reduced to their steady state form. The result is a set of ordinary differential equations that describe hydrodynamic variables and chemical concentrations along the centre of the cylinder. The theory requires specification of the rate of radial expansion, ω_r, as a function of radius. Although Kinetic CHEETAH has implemented three radial expansion models in the code, in this study the simple pressure model with the following time rate of change of ω_r is used:

$$\frac{d\,\omega_r}{dt} = \frac{2SP}{R_o^2 \rho_o} - S\,\omega_r^2 \tag{1}$$

where

$$\omega_r(t=0) = (D_s - u)/R_c \tag{2}$$

Here, P is the pressure, u is the particle velocity in the shock frame, ρ_o is the initial density of the explosive, R_o is the charge radius and S is an empirical scaling factor. If this model is used with $S = 0$, ω_r is a constant with the initial value determined by the radius of curvature R_c, the detonation velocity D_s, and the particle velocity at the detonation front. The radius of curvature is obtained from Souer's detonation front curvature and size effect data [Souers 1998].

Kinetic CHEETAH assumes the concentrations of individual reactants are controlled by the rate of the kinetic reactions, while the products are assumed to be in thermochemical equilibrium. Kinetic CHEETAH supports multiple reaction rate laws:

- Simple constant reaction rate law
- Simple Arrhenius kinetics with a temperature-dependent pre-factor
- Pressure-dependent rate law
- Hot spot model

A simple constant reaction rate has the form:

$$d\lambda/dt = R(1-\lambda) \tag{3}$$

where R is the rate constant, and λ represents the amount of unburned reactant normalised to vary between zero (all unburned) and one (all burned).

The Arrhenius decay law is :

$$d\lambda/dt = R\,T^A \exp(-B/T)(1-\lambda)) \tag{4}$$

where T is the temperature, R and B are the rate constants, and A is the temperature exponent.

A pressure-dependent rate law describing surface controlled reaction has the form:

$$d\lambda/dt = R\,\lambda^A\,(1-\lambda)^{B+1}\,P^D \tag{5}$$

where P is the pressure, R is the rate constant, A and B are the extent of reaction exponents, and D is the pressure exponent.

The hot spot model has the form:

$$d\lambda/dt = R\,\lambda^A\,(1-\lambda)^{B+1}\,P^D\,f \tag{6}$$

$$df/dt = E\,(1-f)\,\exp\left(-C/T_{hotspot}\right) \tag{7}$$

where E and C are constants, and f represents the degree of reaction of hot spots.

CHEETAH has used the following simple pressure-dependent rate law to infer kinetic rates for a variety of high explosives and their composites:

$$d\lambda/dt = (1-\lambda)\,R\,P^D \tag{8}$$

We have also used the same rate law in our study. By using the NEWC1 product library and the updated rate constant values for the pressure exponent D of 2 as defined by Howard et al. [1998], rather than those rate constants initially recorded in the CHEETAH 2.0 User's Manual, we have computed the reaction zone widths over a wide range of charge radius, and these results are presented in Table 1. Souers [1999] proposed a dimensionless relation $N = x_e/R_0$ to measure the non-ideality of explosives (where x_e is the reaction zone). For an ideal explosive, $N = 0$. The larger N gets, the more non-ideal the explosive becomes. For $N > 0.3$, the explosive is extremely non-ideal. According to this definition, PBXW-115 can be classified as extremely non-ideal for $R_o \leq 24.8$ mm, moderately non-ideal for 24.8 mm $\leq R_o \leq 85$ mm and mildly non-ideal for $R_o \geq 100$ mm (see Table 1).

Table 1. Reaction zones calculated from Kinetic CHEETAH

Charge radius R_0 (mm)	Time to sonic point (μs)	Reaction zone x_e (mm)	$N = x_e / R_0$
19.35	1.315	6.786	0.351
20.55	1.288	6.814	0.332
24.8	1.279	7.072	0.285
34.55	1.291	7.410	0.214
49.95	1.347	7.917	0.159
65	1.370	8.173	0.126
75	1.361	8.160	0.109
85	1.455	8.759	0.103
100	1.498	9.054	0.091

Using the same rate constants with the pressure exponent D=2, we also calculated the detonation velocities as a function of reciprocal of radius of curvature. Figure 1 summarises the predicted results with Kinetic CHEETAH, compared with the experimental data [Forbes et al 1989; 1992 and Souers 1998]. It is seen that although CHEETAH can not reproduce exactly the experimental results, it follows a similar trend which demonstrates the diameter effect. The agreement could be improved with further parameter adjustment.

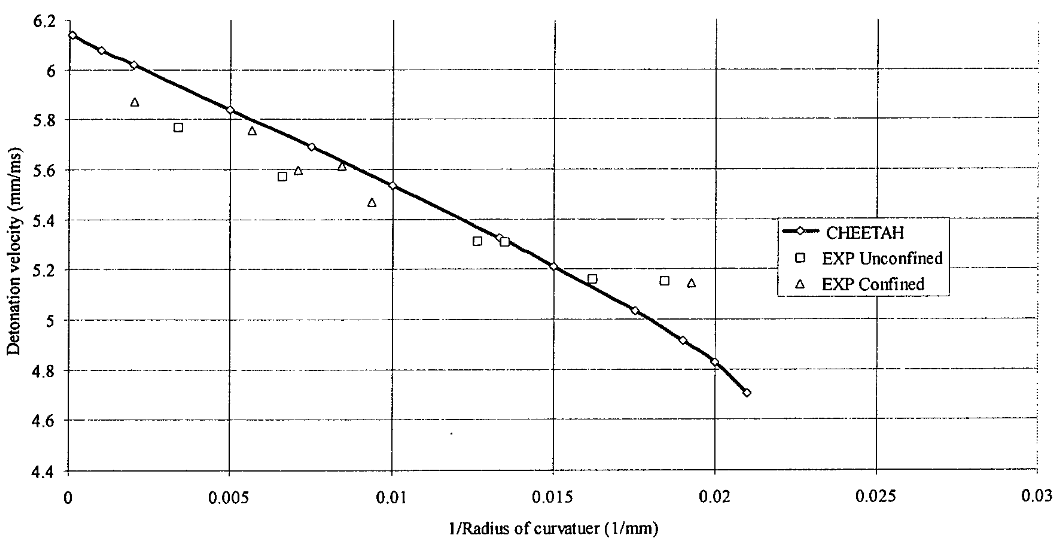

Figure 1 Detonation velocity versus reciprocal radius of curvature of PBXW-115 with D=2

By calibrating kinetic parameters based on the detonation velocity versus diameter effect experimental data for unconfined charges [Forbes et al. 1989; Forbes et al. 1992], we have developed the rate constants by varying the pressure exponent D in the rate law from 2.0 to 1 and 0.5. The rate constants R for the reactants developed in this study

are listed in Table 2. The predicted detonation velocities with the pressure exponent D of 1 and 0.5 together with the experimental data are given in figures 2 and 3. It is seen that the agreement was much improved by decreasing the pressure exponent D in the rate law from 2.0 to 0.5. Northam and Jessee [1969] conducted experimental investigations of the effect of aluminium size and loading on the burning rate of solid propellants (AP/Al/curing agents) under various acceleration loads. At each acceleration level the average burning rates were fitted by the least-squares method to Vieille's burning rate law ($r=a\ (P/500)^n$, where r is the average burning rate over pressure action time in mm/s, n is the pressure exponent, P is the average chamber pressure in N/m^2 and a is a constant). The pressure exponent n resulted from the data fit ranged from 0.239 to 0.491. Their experimental data lend some support to the square root pressure dependence providing a better fit to the detonation velocity data than the pressure exponent of either 1.0 or 2.0.

Table 2. Rate constant R used in pressure-dependent rate laws

Reactant	R ($\mu s^{-1}GPa^{-2}$)		
	$D=2$	$D=1$	$D=0.5$
Al	0.0075	0.084375	0.3
AP	0.0075	0.084375	0.3
HTPB	0.001	0.01125	0.04
RDX	0.2	2.25	12.5

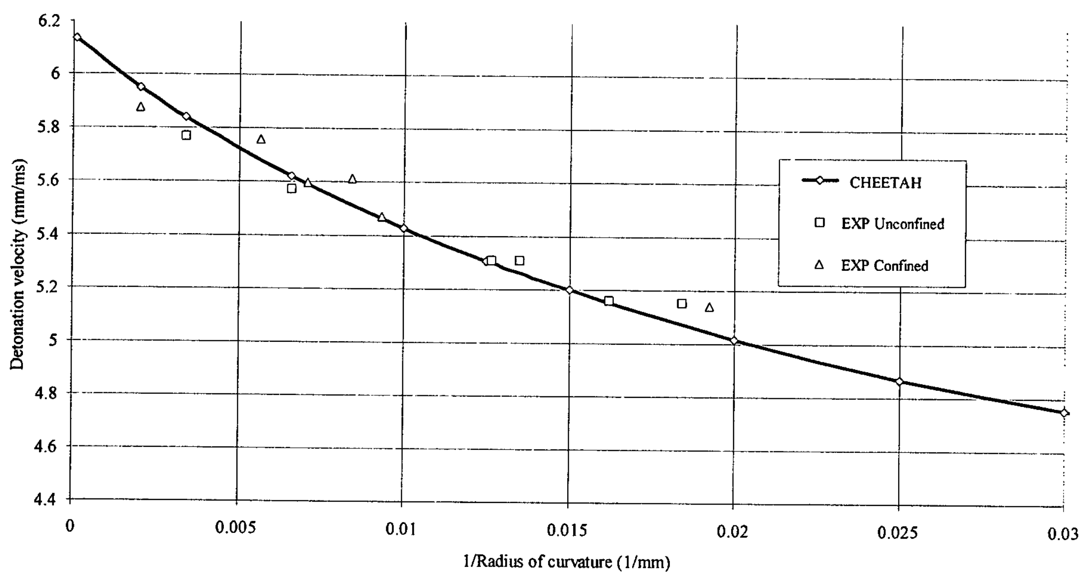

Figure 2 Detonation velocity versus reciprocal radius of curvature of PBXW-115 with D=1

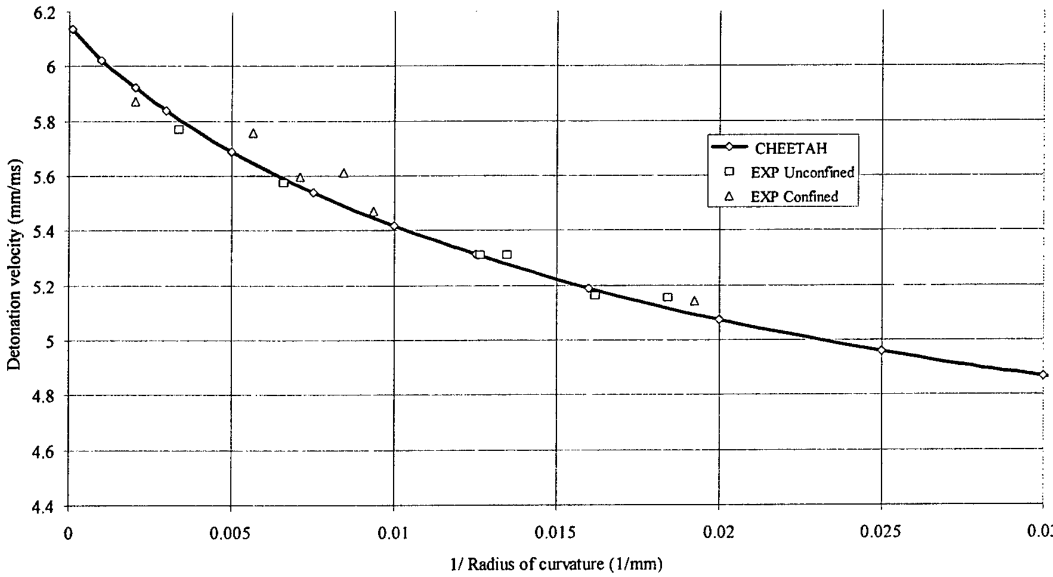

Figure 3 Detonation velocity versus reciprocal radius of curvature of PBXW-115 with D=0.5

Preliminary modelling results conducted by the second author indicate that the detonation velocity and the critical diameter are sensitive to the assumed AP decomposition rate. Although this might suggest that the observed differences between the US and the Australian composition are due to the particle size of the AP rather than the RDX, it is worth noting that the recent study on the effect of Australian RDX on PBXN-109 performances [Lochert et al 2002] indicated that the above differences (large critical diameter and improved shock sensitivity) were also present in PBXN-109 (which has no AP). To clarify the role of AP, further investigation of the effects of the assumed AP decomposition rate on the detonation velocity as a function of charge diameter will be required in the future.

3. Hydrocode Modelling

3.1 Ignition and growth reactive model in LS-DYNA

The Ignition and Growth (I & G) Reactive Model in LS-DYNA[1999] is derived from the original work of Lee and Tarver [1980], which permits the resolved reaction zone simulation of initiation (or failure to initiate) and detonation wave propagation of solid high explosives. According to Tarver et al. [1985], shock initiation of heterogeneous solid explosives should be modelled as at least a three-step process. The first step is the formation of hot spots created by various mechanisms (void closure, viscous heating, shear banding, etc.) during shock compression and the subsequent ignition (or failure

to ignite due to heat conduction losses) of these heated regions. The second step in the process is assumed to be a relatively slow growth of reaction in inward and/or outward "burning" of the isolated hot spots. The third step in the shock initiation process is a rapid completion of the reaction as the reacting hot spots begin to coalesce. This model requires [Murphy et al. 1993]:

- An unreacted explosive equation of state;
- A reaction product equation of state;
- A reaction rate law that governs the chemical conversion of explosive molecules to reaction product molecules;
- A set of mixture equations to describe the states attained as the reactions proceed.

Both unreacted and product equations of state are of Jones-Wilkins-Lee (JWL) forms

$$P = Ae^{-R_1 V} + Be^{-R_2 V} + \frac{\omega C_v T}{V} \tag{9}$$

where P is pressure, V is relative volume, T is temperature, and A, B, R_1, R_2, ω (the Gruneisen coefficient) and C_v (the average heat capacity) are constants. The chemical reaction rate equation in the three-term ignition and growth model is of the form [Tarver and Green 1989]:

$$\frac{\partial F}{\partial t} = I(1-F)^b \left(\frac{\rho}{\rho_0} - 1 - a\right)^x + G_1(1-F)^c F^d P^y + G_2(1-F)^e F^f P^z \tag{10}$$

where F is the fraction reacted, t is time, ρ_0 is initial density, ρ is current density, P is pressure, and I, G_1, G_2, b, x, a, b, c, d, y, e, f, and z are constants. Three more constants are added to the model: F_{mxig}, F_{mxGr} and F_{mnGr} which limit the contributions of the three terms to respectively a maximum reacted fraction F_{mixg} for the first term, a maximum fraction F_{mxGr} for the second term and a minimum fraction F_{mnGr} for the last term.

It is known that the mesh size significantly influences the prediction accuracy. The mesh size dependency of the model with different mesh densities were examined. Considering both the factors of computing time and accuracy, an element size of 1mm for explosives and 2mm for water was required to model the experiment correctly, giving close to 8 mesh points through the reaction zone.

Table 3 lists the parameters in the Ignition and Growth Reactive Model fitted to experimental data for the detonation velocity versus diameter for unconfined PBXN-111 [Forbes 1989] and PBXW-115 (*Aust*) [Bocksteiner et al. 1994]. Figure 4 summarises the LS-DYNA predictions and kinetic CHEETAH predictions of detonation velocity in axisymmetric geometry, together with experimental data. Agreement is seen to be excellent between the DYNA predictions and the experimental results for both PBXW-115 (*Aust*) and PBXN-111 (US). The curve predicted by LS-DYNA and that predicted by

CHEETAH follow similar trends. As mentioned earlier, even though CHEETAH overestimates the detonation velocities, it can still predict the trend of the detonation velocity versus diameter effect.

Table 3. Parameters for the Ignition and Growth of Reaction Model [Lu et al 2002]

Explosive	PBXN-111	PBXW-115(Aust)
Unreacted Equation of State and Constitutive Values		
ρ_0 (g/cm^3)	1.792	
A (GPa)	4.066E+03	
B (GPa)	-133.9	
R_1	7.2	
R_2	3.6	
$R_3=\omega * C_v$ (GPa/K)	2.091E-03	
Yield Strength (GPa)	0.2	
Shear Modulus (GPa)	4.54	
Reacted Product Equation of State and CJ Values		
A (GPa)	372.9	
B (GPa)	5.412	
R_1	4.453	
R_2	1.102	
$R_4=\omega * C_v$ (GPa/K)	4.884E-04	
E_o (kJ/cc)	12.95	
D_{cj} (mm/µs)	6.476	
P_{cj} (GPa)	20.84	
Reaction Rate Parameters for 3 Term Model		
I (µsec^{-1})	30	15
b	0.6667	0.6667
a	0	0
x	4.0	4.0
G_1 (GPa^{-y}µsec^{-1})	0.045	0.0195
c	0.6667	0.6667
d	0.1111	0.1111
y	1.0	1.0
G_2 (GPa^{-z}µsec^{-1})	1.805E-03	8.00E-04
e	1.0	1.0
f	0.1111	0.1111
z	2.0	2.0
F_{mixg}	0.015	0.015
F_{mxGr}	0.25	0.25
F_{mnGr}	0	0

Note: E_o is the internal energy.

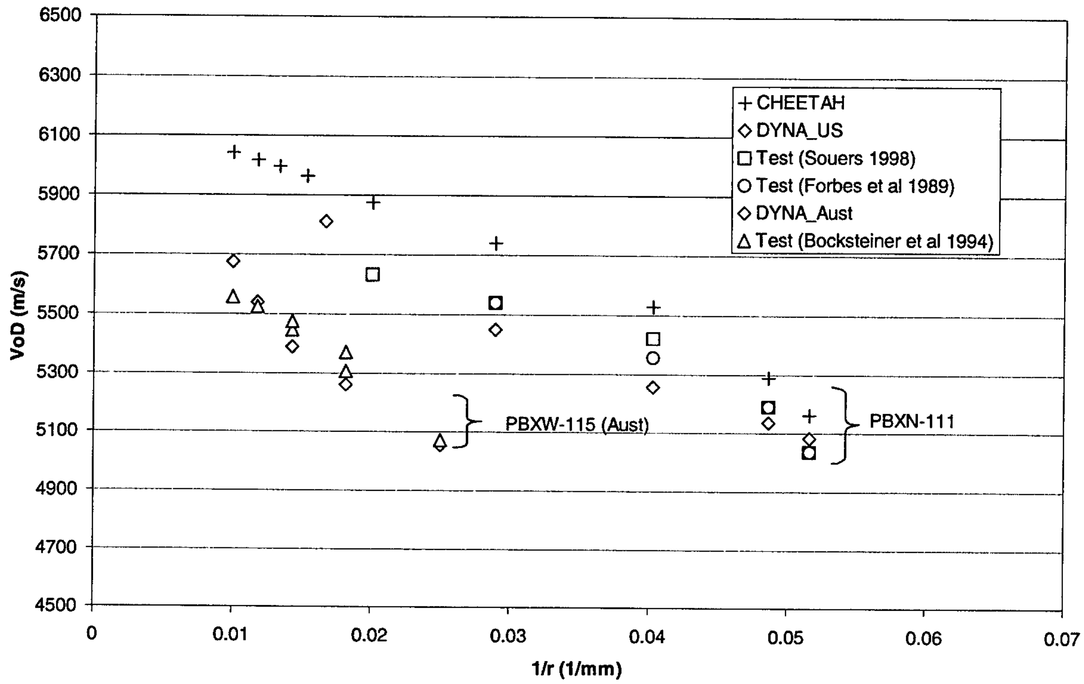

Figure 4 PBXW-115 Detonation velocity for unconfined charges

3.2 CPeX reaction model

The CPeX (Commerical Performance of eXplosives) Reaction Model is based upon the Wood-Kirkwood theory of slightly divergent detonation. Like the Ignition and Growth model, this model also involves a three-stage process to describe varying rates of combustion among the ingredients of a composite explosive. It describes the flow along the central streamtube between the detonation front and the CJ plane for unconfined cylindrical geometry. There are four adjustable parameters – three characteristic reaction times (hotspot, intermediate and final stages of the reaction) and the critical pressure that inhibits the onset of the hotspot reaction, which can be calibrated against the experimentally observed dependence of detonation velocity on charge diameter. For both PBXN-111 and PBXW-115(*Aust*), these parameters are based on the assumption of the initial ignition and consumption of the RDX, the intermediate decomposition of the AP plus binder, and the later reaction of the Al. The CPeX model has been incorporated into both the explicit finite difference two-dimensional in-house multi-material Eulerian hydrocode "MULTI" [Jones et al 1998] and the explicit finite element hydrocode DYNA2D [Kennedy and Jones 1993] to permit the simulation of time-dependent reactive flow in non-ideal explosives.

3.3 Simulations of detonation front curvature

The detonation velocities of highly non-ideal explosives can show large departures from the ideal detonation velocities predicted from thermodynamic equilibrium codes (Kennedy 1998). This is due to detonation waves in non-ideal composite explosives having curved wave fronts resulting from the reacting explosive having a finite size, a varying energy release rate, and hydrodynamic flow [Forbes et al 1992]. Knowledge of the variation of shock front curvature with charge diameter is important in that it is basic data for validation and use of detonation models [Leiper and Hackett 1997]. Experimental wave curvature data for PBXW-115(*Aust*) is not yet available; herein the LS-DYNA simulations of shock front curvature for both PBXN-111 and PBXW-115(*Aust*) unconfined charges using Ignition and Growth Reactive Model are presented, where the simulated results for PBXN-111 are compared with the available experimental data [Forbes et al 1992; Lemar and Forbes 1994]. Analogy between the two versions of this explosive is expected.

Although the detonation front locus can be fitted to many forms, such as circles, second order polynomials, ellipses and the natural logarithm of a Bessel function [Kennedy 1998], herein two forms are chosen to fit the simulated locus. The first is an ellipse in the form [Kennedy 1998]

$$L(R) = b\left\{1-\sqrt{1-\left(\frac{R}{a}\right)^2}\right\} \tag{11}$$

where R is the radial coordinate along the charge radius (see Figure 5), L the detonation lag along the axis of the cylindrical charge (see Figure 5), and a and b are fitting constants for a given radius. The second is the equation described by Souers and Raul [1997]

$$L(R) = a\,R^2 + b\,R^6 \tag{12}$$

The fitted results of the simulations for PBXN-111 together with the experimental results are shown in Figure 6. The scatter indicates the difficulty in measuring the wave front curvature experimentally. It is seen that the curves simulated using both equations (11) and (12) reproduce the experimental data very well. As noted by Miller and Sutherland [1995], the calculated effects at the edges of the charges on the detonation front depend greatly on the grid size used in the hydrocode computations.

Curvature of wave front at any radial coordinate R is defined by

$$\kappa(R) = L''(R) \Big/ \left[1+L'(R)^2\right]^{3/2} \tag{13}$$

The radius of curvature is given by

$$R_c(R) = 1/\kappa(R) \qquad (14)$$

The fit to equations (11) and (12) allows the radius of curvature at any point on the wave front to be computed by Eqs. (13) and (14). The resulting functions for the three PBXN-111 charges are plotted in Figure 7. Similar to the Bessel function fit [Forbes and Lemar 1998], the magnitude of the radius of curvature reaches the maximum at the centre of the detonation wave and then decreases along the radial position.

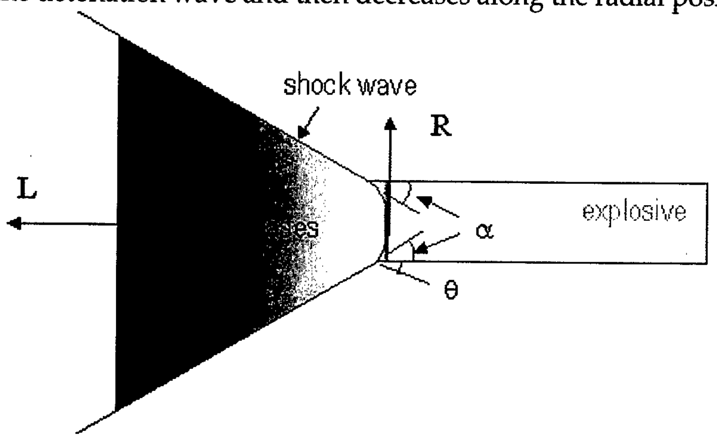

Figure 5 A sketch diagram of a typical rate stick which shows variables L, R, θ and α

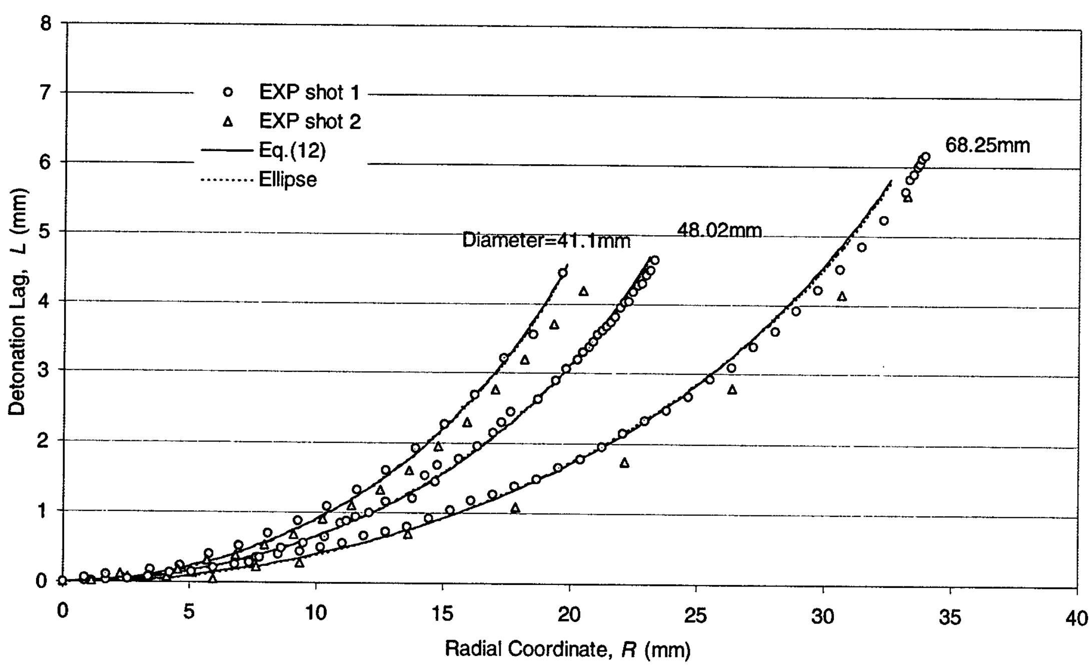

Figure 6 Detonation curvature of PBXN-111

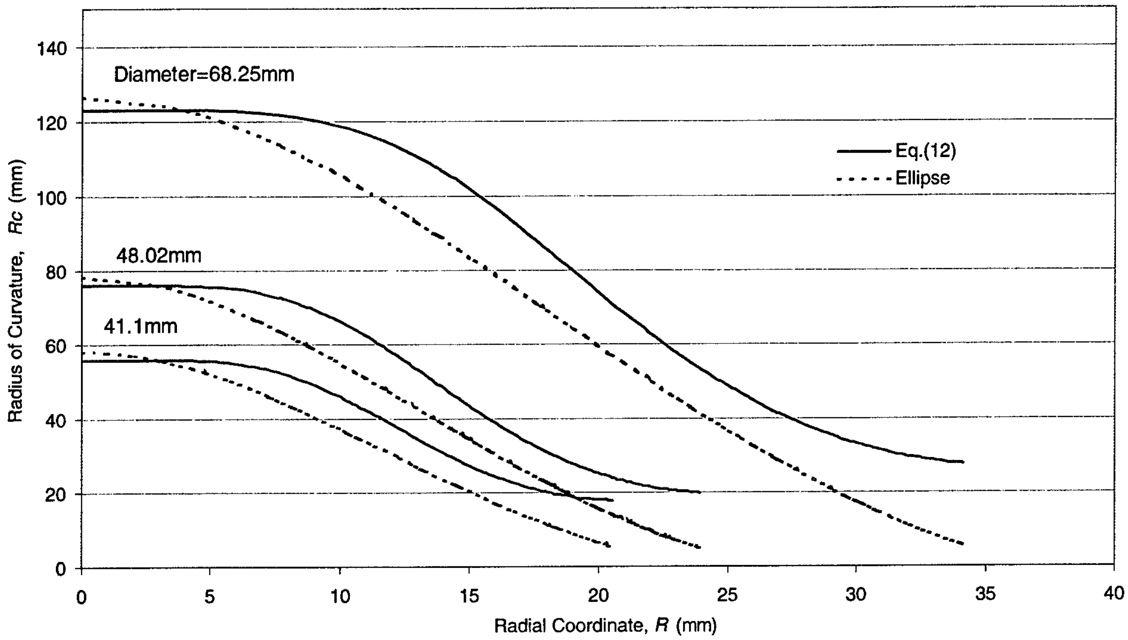

Figure 7 Radius of curvature as a function of radial position for PBXN-111

The angle between the normal to the locus and the axis (see Figure 5), $\theta(R)$, is given by

$$\theta(R)= \arctan(L'(R)) \tag{15}$$

The angle between the detonation wave and the edge of the charge, α, can be determined by two methods. In the first method [Forbes et al 1992], the simulated data over the last 3mm at each edge of the charge are least squares fitted to a straight line to obtain the angles. In the second method, the derivative of either equation (11) or equation (12) is used to obtain the slope of the wave front as given in equation (15), from this, and the angle α (see Figure 5) is calculated by

$$\alpha = 90^o - \theta(R_o) \tag{16}$$

where R_o is the radius of the explosive charge.

The angles at the edges of the charges with different radii, calculated by both methods, and the radii of curvature at the centre of the charges, are summarized in Table 4. For comparison, the experimental data [Forbes et al 1992; Lemar and Forbes 1994] are also included. It is seen that the angles obtained from a linear fit achieve the best correlation with the experimental results. In general, the radii of curvature at the charge centre obtained from an ellipse fit as given in equation (11) results in a better correlation with the experimental data than equation (12), whereas angles obtained from equation (12)

fit give better correlation than those obtained from an ellipse fit. A detailed study on multi-valued normal shock velocity versus curvature relationships for highly non-ideal explosives conducted by Kennedy [1998] showed that it was not straightforward to derive the curvature close to the edges of the charges and the deduced curvature was strongly dependent on the details of the fitting procedure. Although we have attempted to fit the simulated results to a modified elliptical form by a higher order correction term as given in [Kennedy 1998], the correlation has not been improved.

Table 4. Angles of the detonation wave at the edge of the charges and the radii of curvature at the wave centre

Material	Diameter (mm)	α^+ (Deg)	α^* (Deg)	α^{**} (Deg)	$\alpha^\#$ (Deg)	R_c^* (mm)	R_c^{**} (mm)	$R_c^{\#\#}$ (mm)
PBXN-111	41.1	58.9	50.4	53.6	59.1	58.2	55.9	60.65
	48.02	60.5	52.2	57.9	56.9	78.4	76	66.05~73.4
	68.25	60.9	50.8	55.5	60.7	126.4	123	142.6~149.5

+ Obtained from a linear fit of the simulated data at the edge over the last 3mm.

** Obtained from equation (11) fit.*

*** Obtained from equation (12) fit.*

 # Data from [Lemar and Forbes 1994].

Data from [Forbes et al 1992] (R_c =3.18d – 76.30, where d is the charge diameter).

Souers and Garze [1998] presented a simple wave curvature theory to relate curvature with the size effect where they proposed the following formula for calculating the average sonic reaction zone length, χ_e :

$$\chi_e = \frac{R_O(1-U_S/D_\infty)}{\sin(\theta)\cos(\theta)} \tag{17}$$

where R_0 is charge radius, U_s is the detonation velocity and D_∞ is the infinite diameter detonation velocity.

Using equation (17), the zone lengths based on the angles determined with equation (12) are calculated for PBXN-111 and the results are shown in Figure 8. The zone lengths are normalized with respect to charge radius R_0. For comparison, the zone lengths calculated using the angles obtained from experimental data [Lemar and Forbes 1994] for PBXN-111 and those calculated from Kinetic CHEETAH are also included. The agreement is reasonable between the DYNA predictions and the experimental results. Even though CHEETAH underestimates the zone lengths, the curve predicted by LS-DYNA and that predicted by CHEETAH follow similar trends.

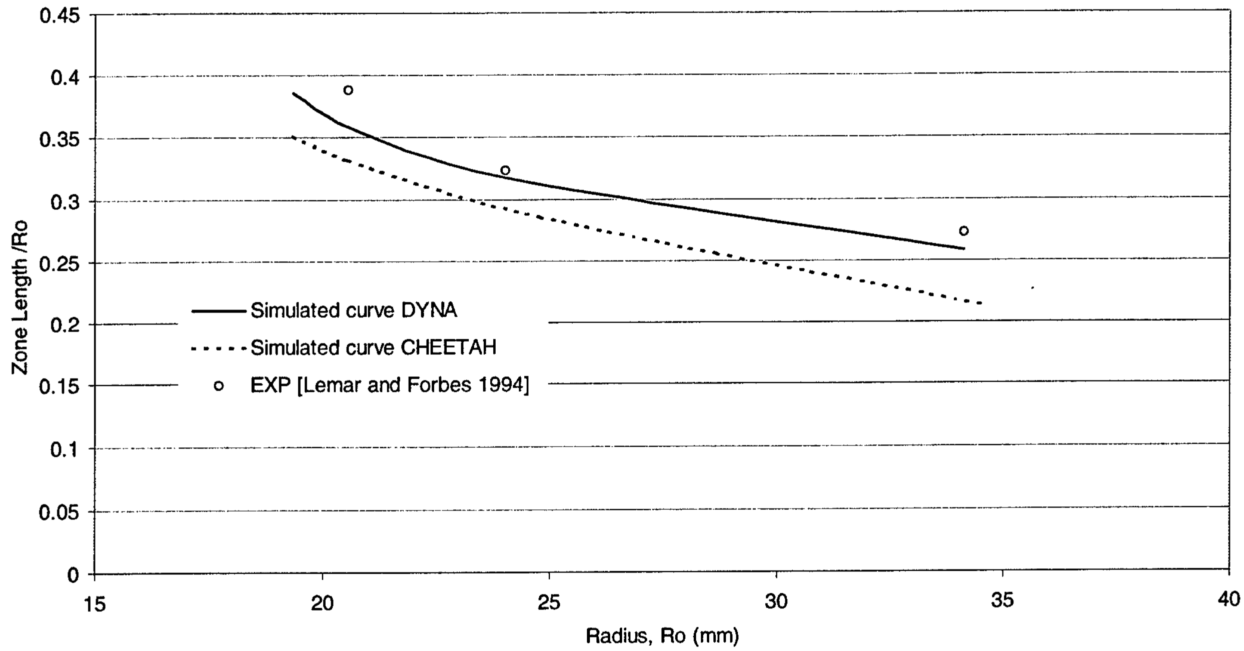

Figure 8 Average sonic reaction zone lengths of PBXN-111

Following the above fitting procedure, the simulated curves of detonation curvature and radii of curvature as a function of radial distances for PBXW-115 (*Aust*) are plotted in Figure 9 and Figure 10, respectively. The angles at the charge edges and the radii of curvature at the charge centres are given in Table 5. Figure 11 shows the detonation velocity as a function of curvature at wave front centres. It is seen that the detonation velocity is sensitive to the curvature of the detonation front. The smaller the charge diameters, the greater expansion and wave curvature, hence result in the lower the detonation velocity. Figure 12 presents the normalized average sonic reaction zone lengths calculated with equation (17).

Given that there is a lack of experimental wave curvature data for PBXW-115(*Aust*), the simulation results presented herein could provide some insight into the detonation process for this non-ideal explosive.

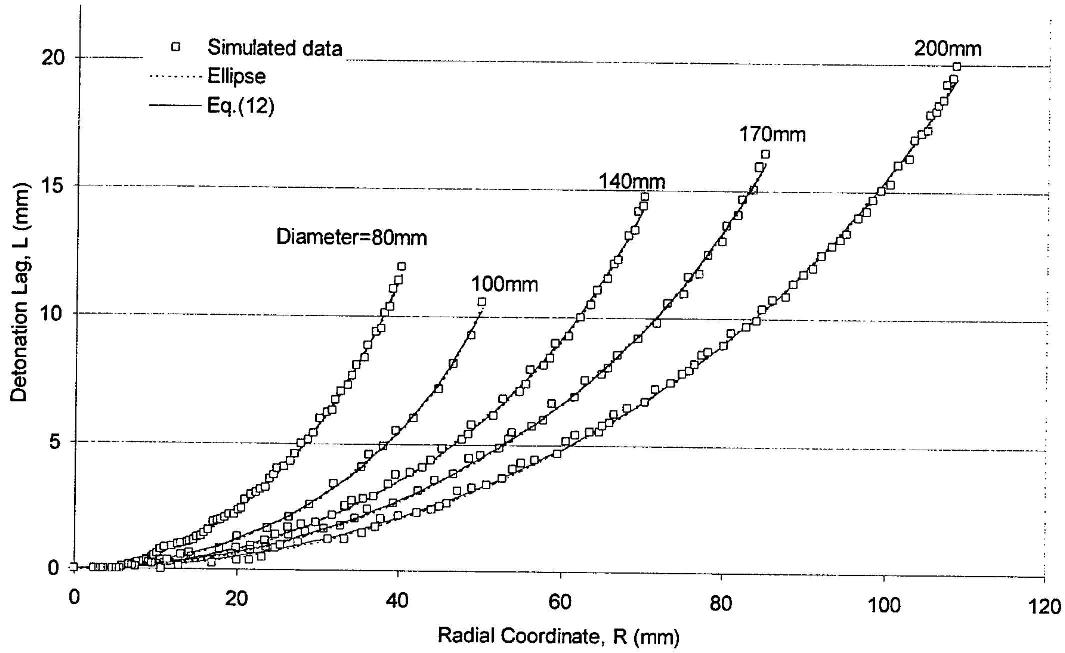

Figure 9 Detonation curvature of PBXW-115 (Aust)

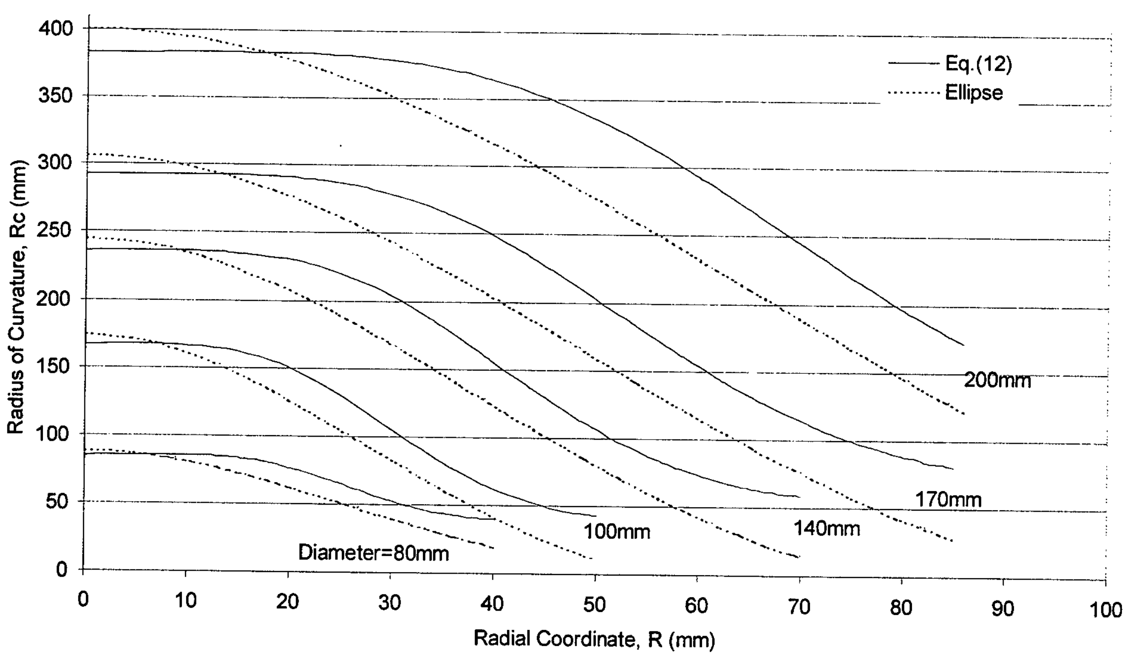

Figure 10 Radius of curvature as a function of radial position for PBXW-115 (Aust)

Table 5. Angles of the detonation wave at the charge edges and the radii of curvature at the wave centre for PBXW-115(Aust)

Material	Diameter (mm)	α^* (Deg)	α^{**} (Deg)	R_c^* (mm)	R_c^{**} (mm)
PBXW-115(*Aust*)	80	51.1	51.5	88.4	84.8
	100	54.3	58.2	173.9	167
	140	59.3	61.4	245	236
	170	59.3	61.4	306	293
	200	62.3	62.6	327.9	313.4

** Obtained from equation (11) fit. ** Obtained from equation (12) fit.*

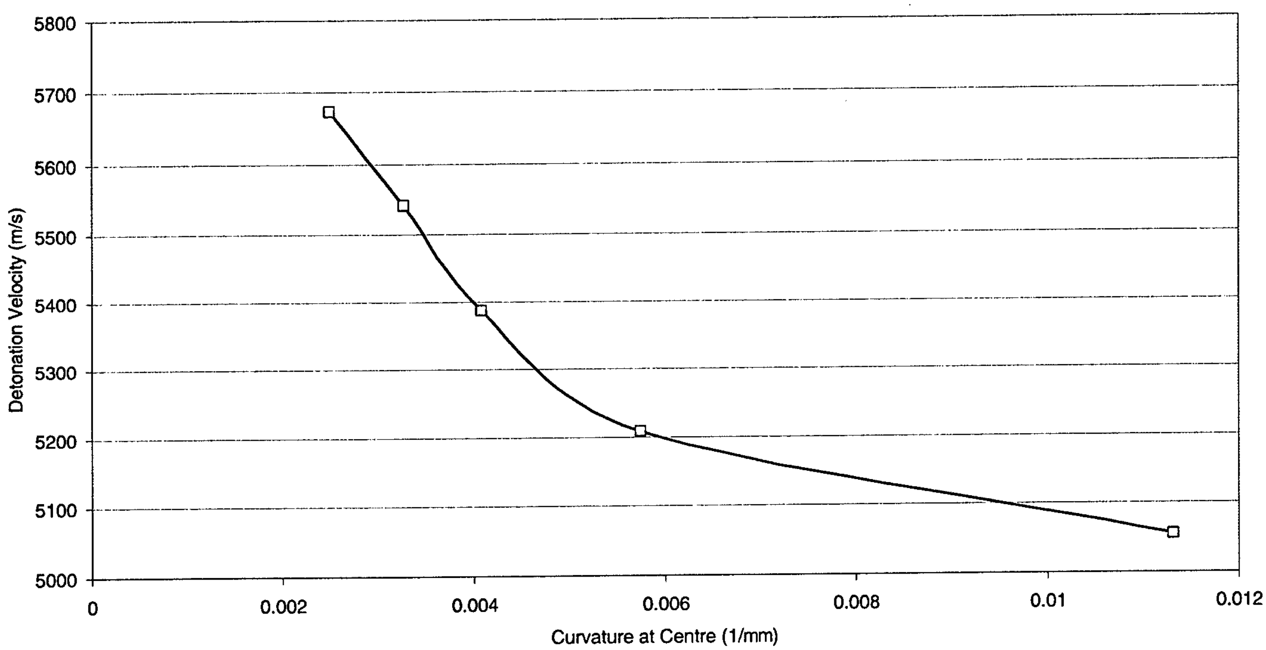

Figure 11 Detonation velocity of PBXW-115 (Aust) as a function of curvature at wave front centres

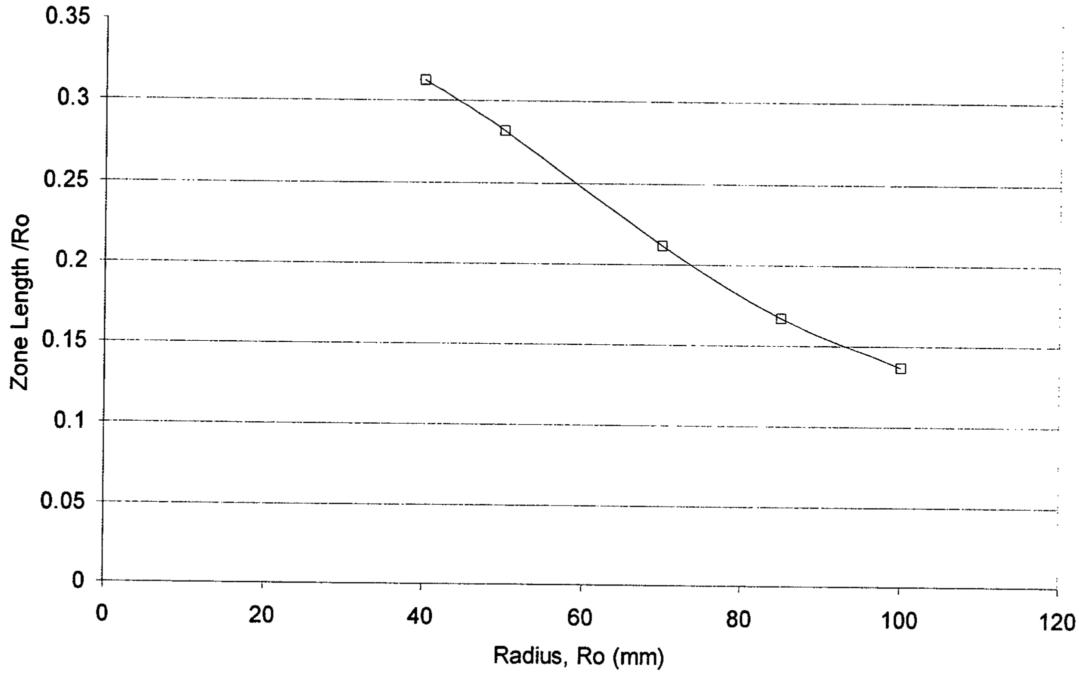

Figure 12 Average sonic reaction zone lengths of PBXW-115 (Aust)

3.4 Modelling of confined charges

Simulating confined charges is difficult. The detonation velocity is sensitive to the curvature of the detonation front. The conditions at the explosive/confinement interface have an influence on the curvature. The element aspect ratio in the confinement should be close to 1 as greater aspect ratios lead to the shock in the confinement travelling faster than it should, and giving too flat a detonation front in the explosive. In order to consider two surfaces in contact it is necessary to designate one as a slave surface and the other as a master surface. Parts in DYNA keyword file are composed of material and section, equation of state and hourglass data. Parts in the slave part set are checked for contact with parts in the master part set. Self contact is checked for any part in both sets. The Ignition and Growth Reactive Model in LS-DYNA and the CPeX Reactive Model in DYNA2D as described previously were validated by comparing their predictions against experimental data [Forbes 1989; Bocksteiner et al. 1994] for detonation of charges confined in 2.5 mm and 3 mm thick brass. Figure 13 demonstrates the I & G model and the CPeX model predictions of detonation velocity in axisymmetric geometry, compared favourably with the experimental data (for confined detonations in both 2.5mm and 3 mm thick brass). Excellent agreement is also seen between the Ignition and Growth Model and the CPeX Model.

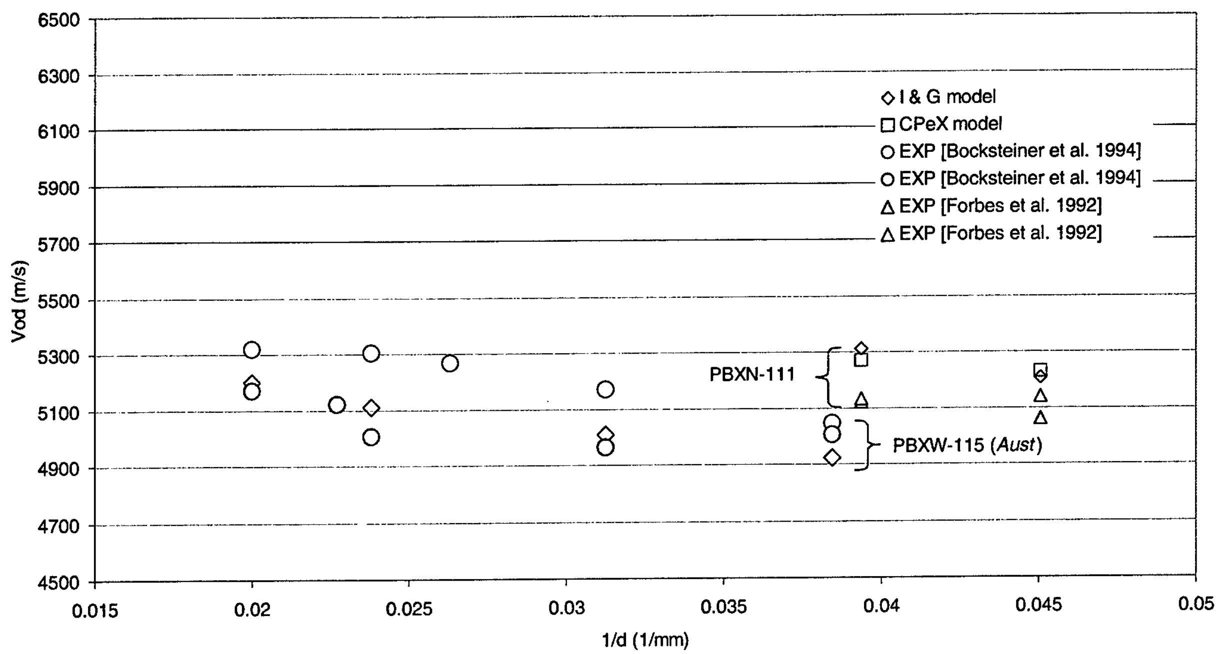

Figure 13 PBXW-115 Detonation velocity for confined charges

3.5 Simulation of aquarium tests

The Ignition and Growth Reactive Model described above has been used to simulate the small-scale aquarium tests reported by Dorsett and Katselis [1999]. The simulation used some 63000 elements in axisymmetric cylindrical geometry with a cell size of 1mm. The PE4 booster was detonated using the programmed burn option in LS-DYNA [1999] with the JWL parameters [Ly 2000] given in Table 6. The PBXW-115 (*Aust*) charge with a diameter of 100mm and a length of 200mm was burnt by the above Ignition and Growth Reactive Model. The surrounding water was modelled with Gruneisen equation of state with the parameters as given in Table 7 [Meyers 1994].

Table 6. JWL parameters for PE4 booster [Ly 2000]

ρ_0 (g/cm^3)	1.59
A (GPa)	774.054
B (GPa)	8.677
R_1	4.837
R_2	1.074
ω	0.284
E_o (KJ/cc)	9.381
D_{cj} (mm/µs)	7.9
P_{cj} (GPa)	24.0

Table 7. Gruneisen parameters for water [Meyers 1994]

ρ_0 (g/cm^3)	1.00
γ_0	0.1
C(mm/μs)	1.65
S	1.92

Note: γ_0 is the Gruneisen gamma, C is the intercept of the shock velocity vs particle velocity curve and S is the coefficient of the slope of this curve .

By tracking the initial high-pressure shock front as it breaks out through the surface of the explosive charge in the modelling results, the apparent detonation velocities were determined and plotted in Figure 14, together with the experimental results [Dorsett and Katselis 1999; Dorsett and Jones 2001]. It is seen that the hydrocode model can reproduce accurately the experimental results.

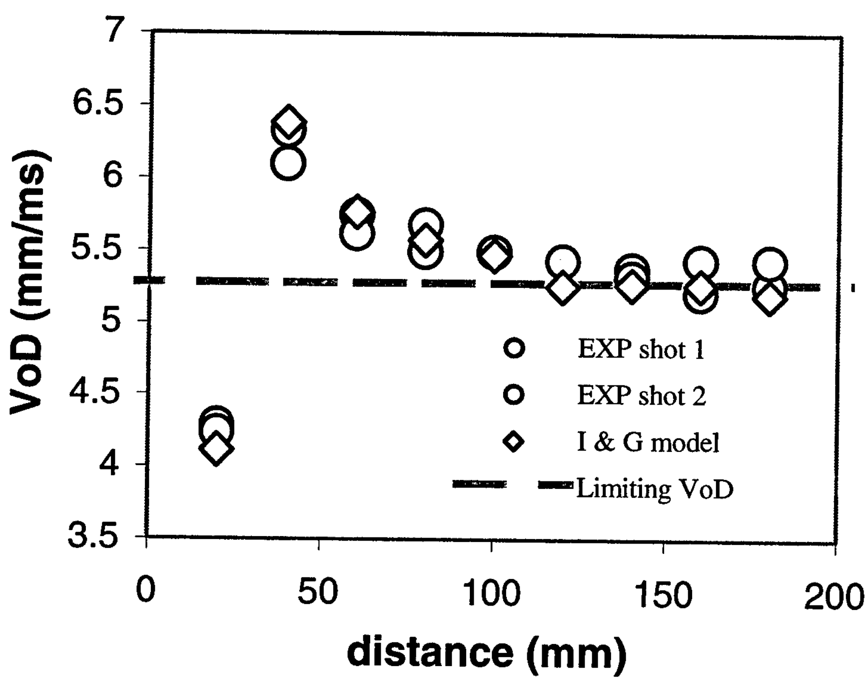

Figure 14. Comparison of predicted and measured apparent detonation velocity along the charge axis

A typical pressure contour plot generated by a LS-DYNA simulation of detonation in water is shown in Figure 15, also showing finite element meshes. Figure 16 presents the results of the simulation after the resolved reaction zone detonation in the PBXW-

115 (*Aust*) has run approximately 32 μs. The calculated contours are of pressure in 1.4 GPa intervals. The positions of the measured shock front and the bubble (explosive/water) interface (after correction for index-of-refraction effects [Craig et al 1978]) are included as open circles [Dorsett and Katselis 1999; Dorsett and Jones 2001]. The results of the simulation after the detonation has run approximately 41 μs and simulated water shock profiles off the end of the charge at 56 μs together with the experimental data are shown in Figures 17 and 18. It is seen that the simulated shock and explosive/water interface are in excellent agreement with the experimental observation.

The good agreement between the hydrocode modelling and experimental observation showed that the Ignition and Growth Reactive Model, although determined from the detonation velocity versus diameter effect experimental data for unconfined explosives, could faithfully model the reaction rate characteristics for experiments carried out in other configurations. This gives us confidence in applying the mentioned models to simulation of the mid-scale underwater tests reported by Wilkinson [2001] which are presented in the following section.

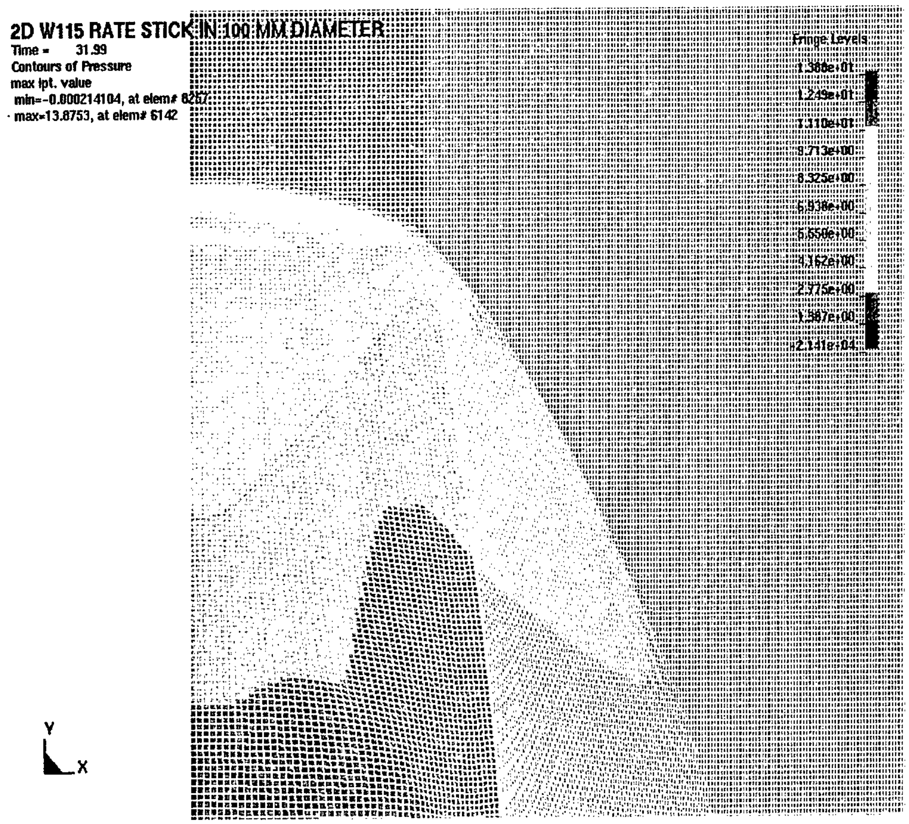

Figure 15 A typical pressure contour plot generated by a LS-DYNA simulation of detonation in water

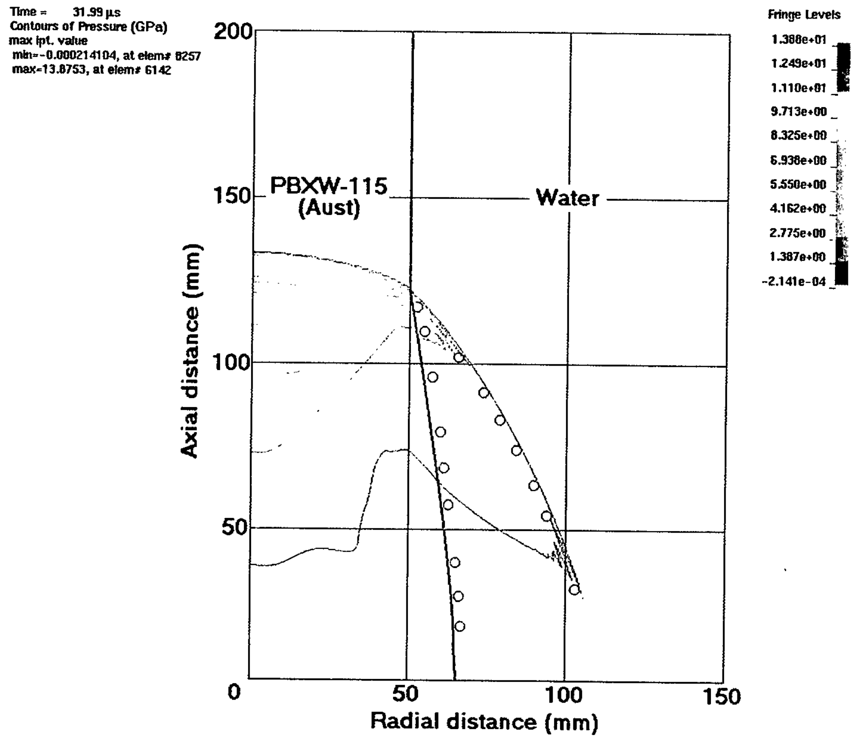

Figure 16. The simulation results by LS-DYNA (solid lines) of the PBXW-115(Aust) aquarium test (open circles represent the experimental data)

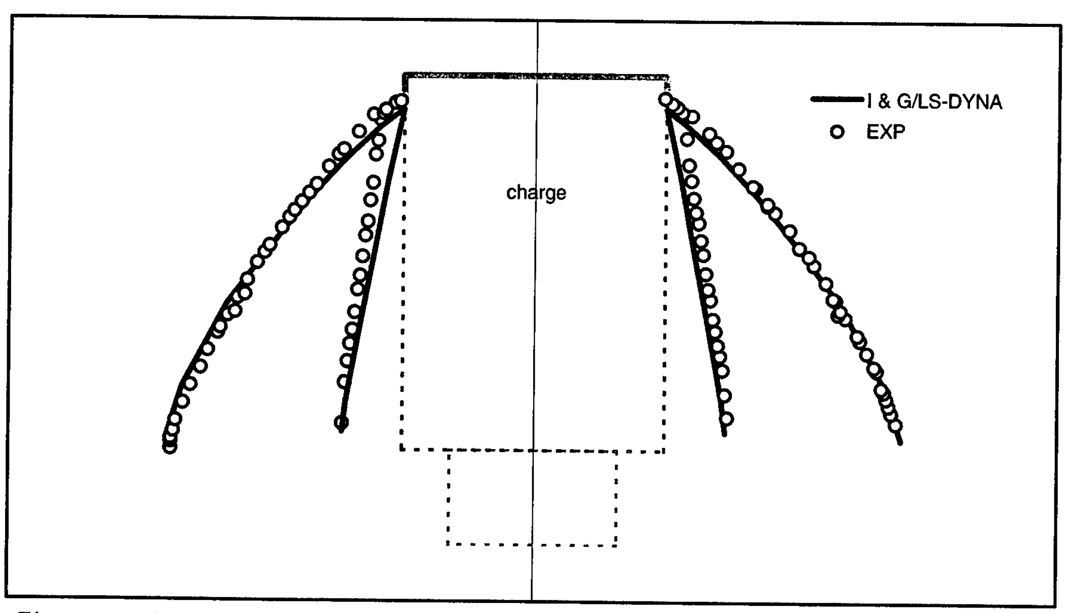

Figure 17. Simulated water shock profiles after the resolved reaction zone detonation has run approximately 41µs (open circles represent the experimental data)

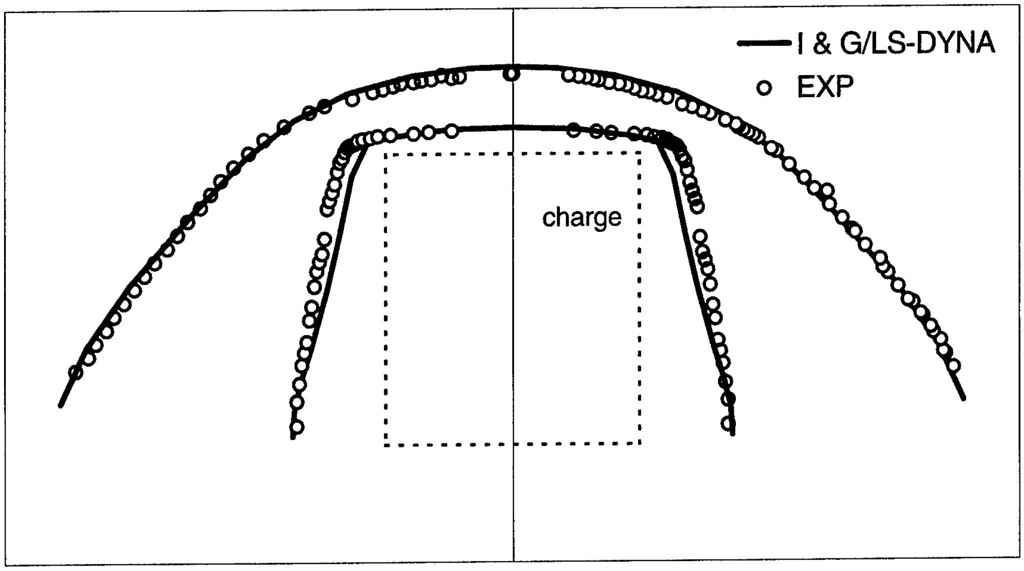

Figure 18. Simulated water shock profiles off the end of the charge at 56µs (open circles represent the experimental data)

3.6 Simulation of mid-scale underwater tests

It is expected that the Ignition and Growth Reactive Model and CPeX Model described above using data from small-scale tests can be applied to large-scale devices. To test this extrapolation, both the Ignition and Growth Model in LS-DYNA and the CPeX Model in DYNA2D [Kennedy and Jones 1993] have been used in the simulation of the mid-scale underwater tests reported by Wilkinson [2001]. Measurement of the underwater explosive performance parameters was obtained through the use of an array of pressure gauges. The gauge stations were placed at 2m, 6m, 11m, 16.5m and 22m. The shock wave similitude equation parameters for peak pressure (P_m) derived by Wilkinson [2001] is given by

$$P_m = 50.4\,Z^{-1.14} \tag{18}$$

where the variable Z represents the scaled distance ($R/W^{1/3}$), R (m) is the distance from the centre of the charge and W (kg) is the charge mass. Note that the similitude parameters are explosive specific and are generally specified for spherical charges with radius of R.

Two configurations were used in the simulations. The first was used to study the initiation process and the intermediate expansion of the water shock and bubble with both the Ignition and Growth Model and the CPeX Model, and the second was used to examine the longer-term effects in underwater detonation with only the Ignition and Growth Model. The size of the first calculation configuration was set to Φ530mm x L1200mm and the second to Φ530mm x L5000mm in axisymmetric cylindrical geometry. The dimensions of the PE4 booster and PBXW-115 charge are 34 and 126

mm in radius and 68 and 400mm in length, respectively. The thickness of the fibreglass confinement case is 9mm. Due to enormous element distortions at later time, the confinement case was not included in the second simulation configuration. The material properties and equations of state for PE4, PBXW-115(*Aust*) and water used in the calculation are the same as those used in the aquarium test simulation. The model parameters for the fibreglass case are given in Table 8. Figure 19 shows the mesh of the model in axisymmetric geometry.

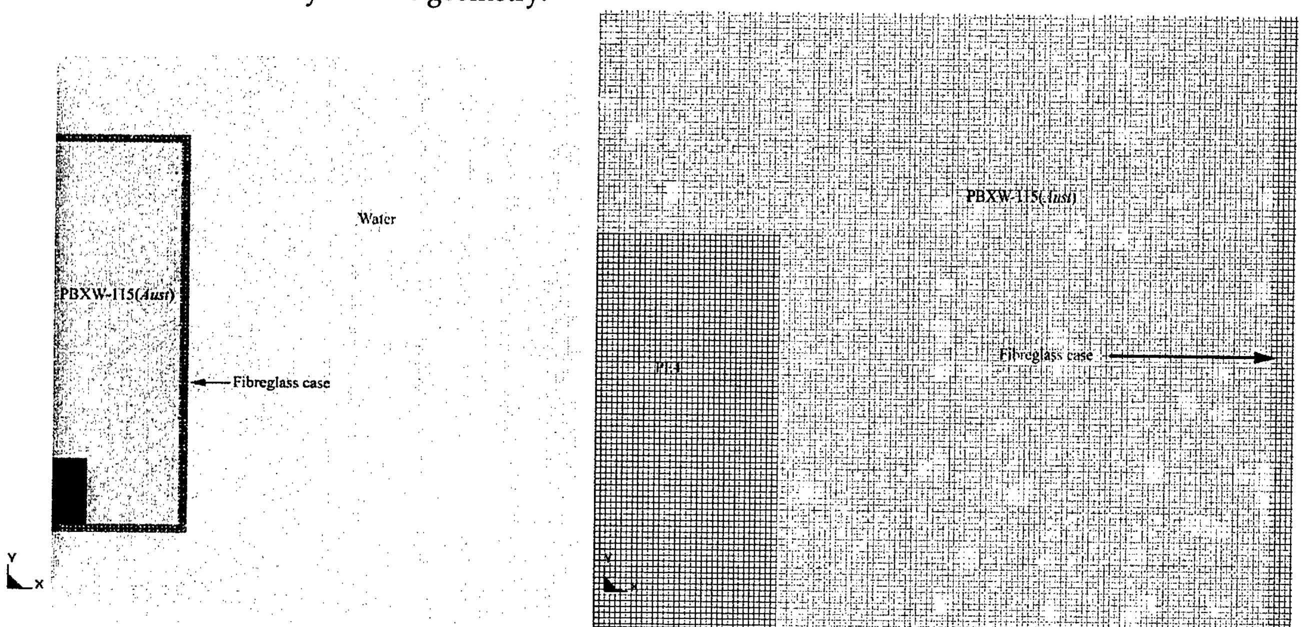

(a) Overall (b) Local enlarged

Figure 19 Geometry and finite element of the model

Table 8. Material and Gruneisen parameters for fibreglass

Yield stress	0.2GPa
Shear modulus	15GPa
ρ_0 (g/cm^3)	1.70
γ_0	1.01
C (mm/μs)	3.016
S	1.005

Figure 20 shows the initiation process and the intermediate expansion of the water shock and bubble. It should be noted that the images from 10 to 80 microseconds are plotted using the linear pressure scale and the images at 120 and 180 microseconds are plotted using a log scale. Good agreement is seen between the Ignition and Growth Model and the CPeX Model. The maximum pressure in the PBXW-115(*Aust*) occurs at the end of the booster, but since the curvature of the resulting detonation wave is too

large for it to be sustained, the shock attenuates down the center line until at about the center of the charge, the shock pressure begins to build up again as its curvature steadily decreases. The detonation propagates most strongly in a 45 degree cone out from the booster, again because of dependence on the curvature.

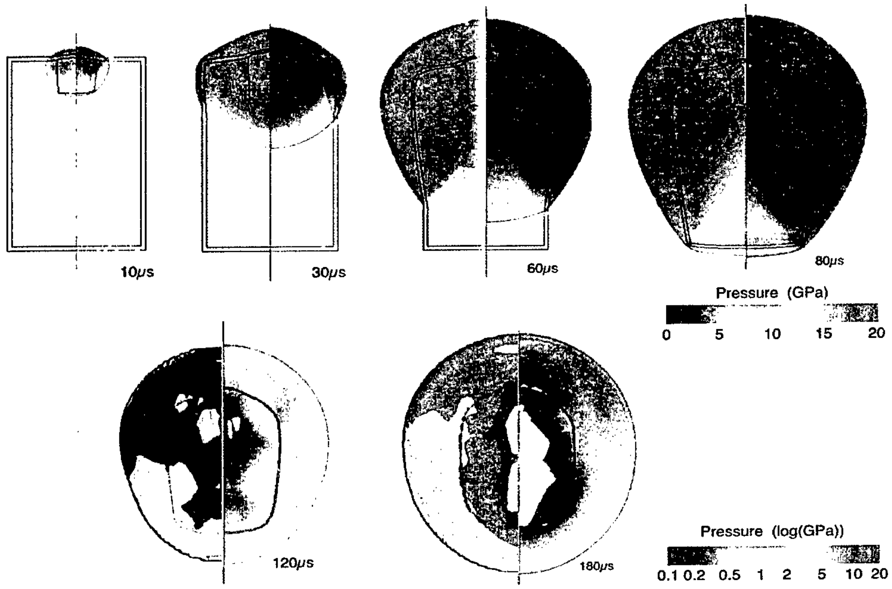

Figure 20. Calculated pressure contours at different times with I & G model plotted on the left side of each diagram while the CPeX model is plotted on the right

Modelling the far field late-time effects of underwater detonation for non-ideal explosives such as PBXW-115 is a challenging task. To this end, to avoid the enormous element distortion, we have removed the inner explosive and water parts when the shock wave passed this portion. Although it is understood that doing so ignores the momentum behind the shock, the smooth transition curve predicted by the Ignition and Growth Model in LS-DYNA as shown in Figure 21 is encouraging. In this way, the problem can run up to 2.49m from the charge centre. For comparison, the peak pressure fitted to equation (18) is also included in the figure. The figure shows peak pressure against scaled distance $Z=L/W^{1/3}$, where L (m), is the distance from the centre of the charge, and W (kg) is the charge mass. There is excellent agreement between the LS-DYNA simulation and the experimental data from the aquarium test [Dorsett and Jones 2001] and mid-scale underwater test [Wilkinson 2001]. This indicates that the Ignition and Growth Model can capture accurately not only the physics of detonation inside the explosives but also the flow properties in the region between the outer boundary of the aquarium and a scaled distance of 0.68. It is worthy of note that there are no published experimental data for peak pressures in this region. Figure 22 plots the calculated peak pressures versus time at the charge edge and in water. The computed peak pressure histories at various locations in the water are repeated for clarity in Figure 23. These figures show the gradual decay in the peak pressure with increasing distance, along with the gradual increase in arrival and duration times.

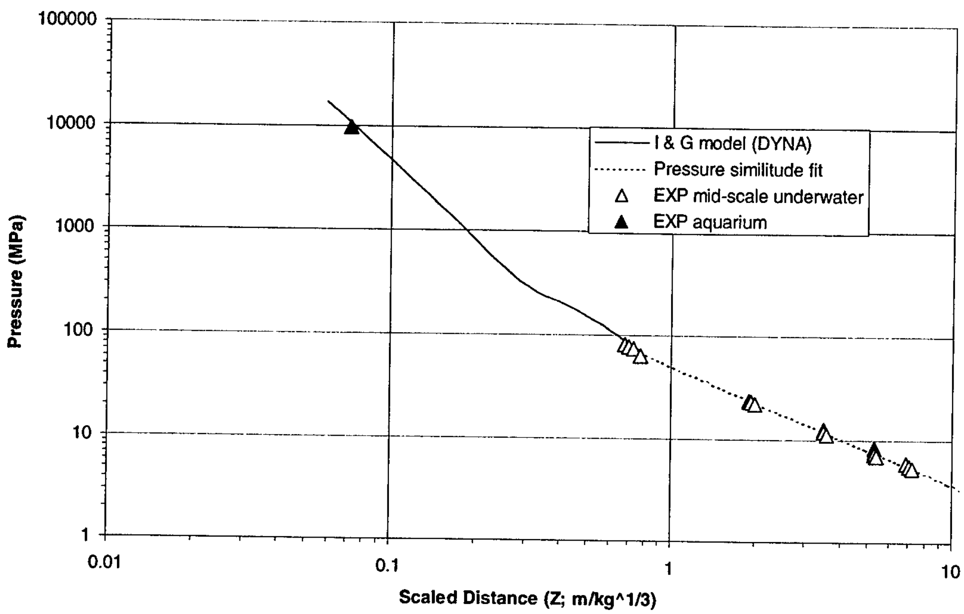

Figure 21. A comparison of predicted peak overpressure with experimental data

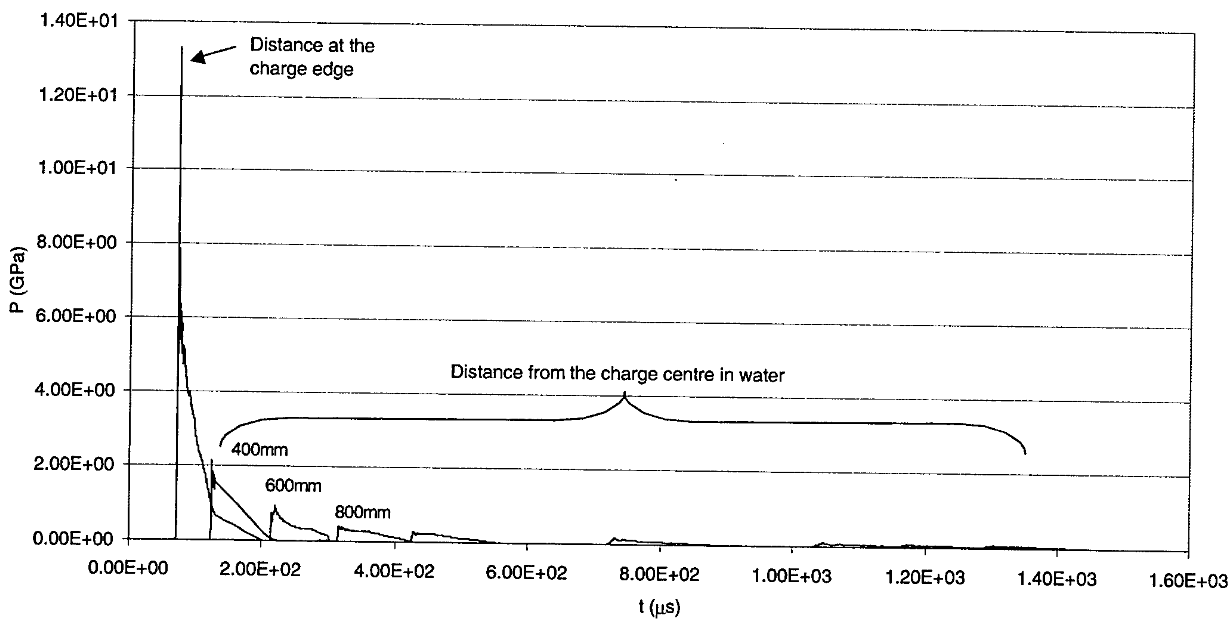

Figure 22 Peak pressure versus time at the charge edge and in water

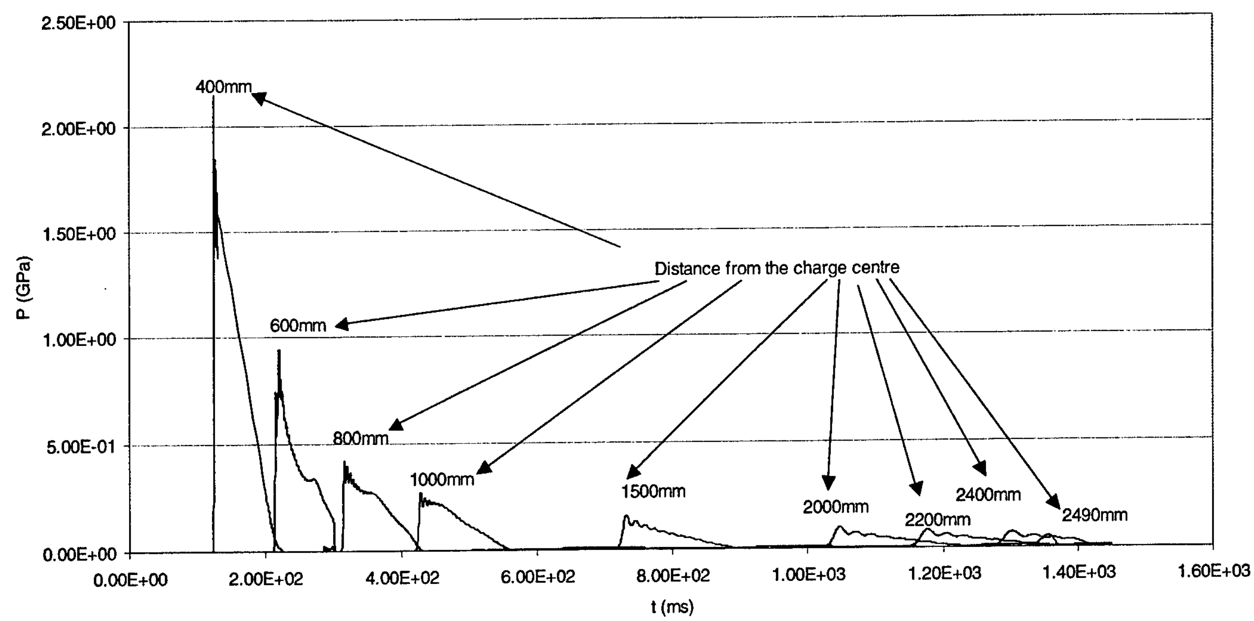

Figure 23 Peak pressure histories at various locations within water

The limitation of the above method is that we deleted the inner portion to get the problem to run without considering the perturbation that is introduced when the elements were deleted. In that way, we generated a rarefaction that will degrade the pressure wave from behind, limiting how far it can run before being totally eroded. Currently we are exploring two other possible approaches to tackle the problem. It would be desirable to set up the problem from the start with three parts, one for the high explosive (HE), one for the inner portion of the water that will be deleted, and one for the outer portion of water that will remain.

The first approach is to run the simulation first and record the pressure time history in an element on the boundary between the inner and outer water. If the HE and inner water are intended to be deleted at time t_1, the first simulation needs to run past t_1, say to t_2 (t_2 is slightly greater than t_1). An exponential function then needs to be fitted to the pressure-time data between t_1 and t_2, in the form

$$P = P_0 \, e^{-A(t-t_1)} \tag{19}$$

where P_o and A are the fitting parameters. We would then have to rerun the simulation setting the termination time to t_1, though now with a *LOAD_SEGMENT_SET applying a pressure load curve to the interface segments between the inner and outer water elements, with the birth time of the load being set to t_1. The pressure-time points for the load curve would then be generated using the function

$$P = P_0 \, e^{-At} \tag{20}$$

When this second simulation stops at t_1, we would then restart it deleting the HE and inner water parts. The pressure boundary will automatically turn on by itself. Obviously, the artificial pressure-time load is not going to be exact all the way along the new boundary (unless the shape of the inner/outer water interface could be matched to a pressure isobar at t_1), but the disturbance should be less than doing nothing at all. If there is a particular direction where it is more important to get the far-field correct, the pressure-time history should be recorded there.

A second way to approach the problem is to switch the HE and inner water to a rigid body at time t_1 using *DEFORMABLE_TO_RIGID_AUTOMATIC. This approach should work best if a right switch time can be picked at which the particle velocities in the HE and the inner water are as low as possible (the final rigid body is given the centre-of-mass velocity of the parts it is replacing).

Work on investigating the above two possible approaches for simulating the far field for late-time effects of underwater detonation using the Ignition and Growth Model is currently underway.

4. Conclusions and Future Directions

From the modelling results presented using kinetic CHEETAH and the simulation results of detonation velocity tests, aquarium tests and the mid-scale underwater tests with the parameters developed for both the Ignition and Growth Reactive Model and CPeX Model, the following conclusions have been reached.

- Kinetic CHEETAH can predict the trend of the detonation velocity versus diameter effect. The square root pressure dependence provides a better fit to the detonation velocity data.
- Preliminary results using kinetic CHEETAH indicate that the detonation velocity and the critical diameter are sensitive to the assumed AP decomposition rate. This might suggest that the observed differences between the US and the Australian composition are due to the particle size of the AP rather than the RDX. Further investigation of the effects of the assumed AP decomposition rate on the detonation velocity as a function of charge diameter will be carried out in the future.
- The Ignition and Growth Reactive Model can capture the physics of detonation inside the explosives accurately, and successfully simulate successive positions of bubble and shock front resulting from a detonation wave propagating down the explosive cylinder observed in the aquarium tests.
- Both the Ignition and Growth Reactive Model and the CPeX model, although determined from the detonation velocity versus diameter effect experimental data for unconfined explosives, could faithfully model the reaction rate characteristics for experiments carried out in other configurations. This has

been validated by comparing the predictions using both models against experimental data for detonation of charges confined in 2.5 mm and 3 mm thick brass.

- The good agreement between the Ignition and Growth Model and the CPeX Model for the simulation of mid-scale underwater tests implies that these two models using parameters derived from small-scale tests could be applied to large-scale devices. We have used a tentative method to model the far field late-time effects of underwater detonation by deleting the inner explosive and water parts when the shock wave passed the portion. Although it is understood that the method ignores the momentum behind the shock without considering the perturbation that is introduced when the elements were deleted, the smooth transition curve predicted between the model and the available experimental peak overpressure data is promising. We have also outlined two other possible approaches. Work on investigating these two possible approaches for simulating the farther field for late-time effects of underwater detonation using the Ignition and Growth Model is currently underway.
- The LS-DYNA simulations of shock front curvature for both PBXN-111 and PBXW-115(*Aust*) unconfined charges using Ignition and Growth Reactive Model are presented, where the simulated results for PBXN-111 are compared with the available experimental data. The average sonic reaction zone lengths for both PBXN-111 and PBXW-115(*Aust*) unconfined charges are calculated based on the simple wave curvature theory by Souers and Garza. Given that there is the lack of experimental wave curvature data for PBXW-115(*Aust*), the simulation results presented herein could provide some insight into the understanding of the detonation process for this non-ideal explosive.
- As part of the program of evaluating the ultrafine aluminium powder 'Alex' in explosive formulations, aquarium tests of Alex-based PBXW-115(*Aust*) will be carried out to measure Alex reaction rates in polymer-bonded explosives. These experimental results, together with the results of VoD and plate dent depth tests and aquarium test of Tritonal (80:20 TNT/Al) explosive formulations containing 'Alex' [Cliff et al 2002], will be used to calibrate the Ignition and Growth model in LS-DYNA to study the role of aluminium and particle size effects.

5. Acknowledgments

The authors would like to acknowledge Dr David A. Jones (MPD) for refereeing the report and many useful suggestions, Dr Helen E. Dorsett (MPD), Dr Farid C. Christo and Dr Con Doolan (WSD) for helpful technical discussions. The work was conducted under Task DST 01/138.

6. References

Anderson, E.W. and Leahy, J.F. (1985) . *Qualification Testing of PBXW-115,* Naval Surface Weapons Center (Maryland, USA) Technical Report NSWC-TR-85-298 (Confidential).

Bocksteiner, G. and Billon, H.R. (1991) *Insensitive Polymer Bonded Main Charge Explosive PBXW-115: Binder and Formulation Studies,* Materials Research Laboratory (Melbourne) Technical Report, MRL TR-91-54.

Bocksteiner, G., Wolfson, M.G. and Whelan, D.J. (1994). *The Critical Diameter, Detonation Velocity and Shock Sensitivity of Australian PBXW-115.* DSTO-TR-0076, AR-008-944, DSTO Technical Report, Melbourne, October.

Bocksteiner, G. (1996) *Evaluation of Underwater Explosive Performance of PBXW-115(Aust),* DSTO Technical Report, DSTO-TR-0297.

Bocksteiner, G., Cliff, M. D. and Horsley, R.A. (1999) *Characterisation of an Insensitive Alternative Explosive Filling for General Purpose Bombs.* DSTO-TR-0761, AR-010-814, DSTO Technical Report, Melbourne, January.

Braithwaite, M., Farran, T., Gladwell, I., Lynch, P.M., Minchinton, A., Parker, I.B. and Thomas, R.M. (1990) *A Detonation Problem Posed as a Differential/Alegbraic Boundary Value Problem,* Math. Engng. Ind., Vol 3, No.1, pp.45-57.

Cliff, M.C., Dorsett, H.E. and Lu, J.P. *Combustion of Nanometric Aluminium in Detonating Solid Explosives,* Presented to the Technical Workshop on The Usage and Performance of Nano-materials, TTCP W-4, held at JHU-APL, Laurel, MD, USA, Feburary-March 2002.

Craig, B.G., Johnson, J.N., Mader, C.L. and Lederman, G.F. *Characterisation of Two Commercial Explosives,* Los Alamos Scientific Laboratory (New Mexico, USA), Technical Report LA-7140, May, 1978.

Dorsett, H. and Katselis, G. (1999) *Detonics Modelling and Testing of IM Explosives,* In PARARI 1999, Proceedings of 4th Australian Explosive Ordnance Symposium, 10 - 12 Nov., Canberra, Australia.

Dorsett, H. E. and Jones, D. A. (2001) *Detonics Modelling and Testing of IM Explosives,* In PARARI 2001, Proceedings of 5th Australian Explosive Ordnance Symposium, 31 Oct. - 2 Nov., Canberra, Australia.

Forbes, J.W., Lemar, E.R. and Baker R.N. (1989) *Detonation Wave Propagation in PBXW-115*, Proceedings of the 9th International Detonation Symposium, Office of the Chief of Naval Research, OCNR 113291-1, pp.806-815.

Forbes, J.W., Lemar, E.R., Sutherland G.T. and Baker R.N. (1992) *Detonation Wave Curvature, Corner Turning and Unreacted Hugoniot of PBXN-111*, NSWCDD/TR-92/164

Forbes, J.W. and Lemar, E.R. (1998) *Detonation Wave Velocity and Curvature of a Plastic-bonded, Nonideal Explosive PBXN-111 as a Function of Diameter and Confinement*, Journal of Applied Physics, Vol. 84, No. 12, 15 December, pp.6600-6605.

Fried, L.E., Howard, W.M. and Souers, P.C. (1998). *CHEETAH 2.0 User's Manual.* UCRL - MA - 117541 Rev. 5, Lawrence Livermore National Laboratory, August.

Hall, T.N. and Holden, J.R. (1988). *Navy Explosives Handbook, Explosion Effects and Properties - Part III. Properties of Explosives and Explosive Compositions.* Research and Technology Department, NSWC MP 88-116, October.

Howard, W.M., Fried, L.E. and Souers, P.C. (1998). *Kinetic Modelling of Non-Ideal Explosives with CHEETAH.* Proceedings of the 11th International Detonation Symposium, Snowmass Village, Colorado, USA, August 31-September 4.

Jones, D.A. and Kennedy, D.L. (1991) *Application of the CPEX Non-ideal Explosive Model to PBXW-115*, Materials Research Laboratory Technical Report, MRL-TR-91-40.

Jones, D.A., Kemister, G. and Borg, R.A.J. (1998). *Numerical Simulation of Detonation in Condensed Phase Explosives*, DSTO-TR-0705, AR-010-605, DSTO Technical Report, Melbourne, August.

Kennedy, D.L. and Jones, D.A. (1993) *Modelling Shock Initiation and Detonation in the Non Ideal Explosive PBXW-115*, Proceedings of the 10th International Detonation Symposium, Boston, Mass., USA, 12-16 July, Office of Naval Research ONR 33395-12, pp. 665-674.

Kennedy, D.L. (1998) *Multi-valued Normal Shock Velocity Versus Curvature Relationships for Highly Non-ideal Explosives*, Proceedings of the 11th International Detonation Symposium, Snowmass Village, Colorado, USA, August 31-September 4.

Kennedy, D. (2000). Orica Explosives, Technical Centre George Booth Drive, Kurri Kurri, New South Wales, Australia, private communications.

Kirby, I.J. and Leiper, G.A. (1985). *A Small Divergent Detonation Theory for Intermolecular Explosives.* Proceedings of the 8th International Detonation Symposium, Albuquerque, pp.176-185.

Lee, E.L. and Tarver C. M. (1980) *Phenomenological model of shock initiation in heterogeneous explosives*, Phys. Fluids, Vol. 23, pp.2362.

Leiper G.A. and Hackett A. (1997) *Shock Front Curvature in Condensed Explosives*, 28th Combus. & Det.

Lemar, E.R. and Forbes J.W. (1994) *Detonation Wave Curvature of Cast Comp B and PBXN-111*, 1994 American Institute of Physics, pp 1385-1388.

Loboiko, B.G. and Lubyatinsky, S.N. (2000) *Reaction Zones of Detonating Solid Explosives*, Combustion, Explosion, and Shock Waves, Vol.36, No. 6, pp.716-733.

LS-DYNA Keyword User's Manual, Nonlinear Dynamic Analysis of Structures, May 1999, Version 950, Livermore Software Technology Corporation.

Lu, Jing Ping (2001) *Evaluation of the Thermochemical Code – CHEETAH 2.0 for Modelling Explosives Performance*, DSTO-TR-1199, AR-011-997, DSTO Technical Report, Melbourne, August.

Lu, J.P. and Kennedy, D.L. (2001) *Modelling of non-ideal explosive PBXW-115*, In PARARI 2001, Proceedings of 5th Australian Explosive Ordnance Symposium, 31 Oct. – 2 Nov., Canberra, Australia.

Lu, J.P. , Dorsett, H. and Kennedy, D.L. (2002) *Simulation of Aquarium Tests for PBXW-115(Aust)*, Proceedings of the 12th International Detonation Symposium, San Diego, California, USA, 11-16 August.

Ly, E. (2000), a former employee in Terminal Effect Group, WSD, DSTO, Salisbury, Private Communication.

Meyers, M. A.(1994), *Dynamic Behavior of Materials*, John Wiley & Sons, Inc.

Miller, P.J. and Sutherland G.T. (1995) *Reaction Rate Modelling of PBXN-110*, Shock Compression of Condensed Matter – 1995, August 13-18.

Miller, P.J. (1996a) *A Simplified Method for Determining Reactive Rate Parameters for Reaction Ignition and Growth in Explosives*, Mat. Res. Soc. Symp. Proc. Vol. 418, pp.325-330.

Miller, P.J. (1996b) *A Reactive Flow Model with Coupled Reaction Kinetics for Detonation and Combustion in Non-ideal Explosives*, Mat. Res. Soc. Symp. Proc. Vol. 418, pp.413-420

Miller, P.J. and Guirguis R.H.(1996) *Experimental Study and Model Calculations of Metal Combustion in Al/AP Underwater Explosives*, Mat. Res. Soc. Symp. Proc. Vol. 418, pp.299-303.

Murphy, M.J., Lee E.L., Weston, A.M. and Williams, A.E.(1993) *Modeling Shock Initiation in Composition B*, Proceedings of the 10th International Detonation Symposium, Boston, Mass., USA, 12-16 July, Office of Naval Research ONR 33395-12, pp.963-970.

Northam, G.B. and Jessee, W.P. (1969) *Experimental Investigation of the Effect of Aluminium Size and Loading on the Burning Rate of Solid Propellants under Acceleration*, NASA TN D-5397, NASA Technical Note, National Aeronautics and Space Administration, Washington, D.C., September.

Souers P. C. (1997) *Size Effect and Detonation Front Curvature*, Propellants, Explosives, Pyrotechnics 22, 221-225.

Souers P. C. (1998) A *Library of Prompt Detonation Reaction Zone Data*, UCRL-ID-130055 Rev 1, June, Lawrence Livermore National Laboratory.

Souers P. C. and Garza R. (1998) *Kinetic Information from Detonation Front Curvature*, Proceedings of the 11th International Detonation Symposium, Snowmass Village, Colorado, USA, August 31-September 4.

Souers P. C. (1999) *Measuring Explosive Non-ideality*, Proceedings of 1999 International Workshop on the modelling of Non-Ideal Explosives Energetic Materials Research and Testing Center, New Mexico Institute of Mining and Technology, Socorro, NM, 16-18 March.

Souers P. C., Forbes J.W., Fried L.E., Howard W.M., Anderson S., Dawson S., Vitello P. and Garza R. (2001) *Detonation Energies from the Cylinder Test*, Propellants, Explosives, Pyrotechnics 26, 180-190.

Tarver, C.M., Hallquist, J.O. and Erickson, L.M. (1985) *Modeling Short Pulse Duration Shock Initiation of Solid Explosives*, Proceedings of the 8th International Detonation Symposium, Naval Surface Weapons Center, Albuquerque, NSWC MP 86-194, pp.951-961.

Tarver C.M. and Green L.G. (1989) *Using Small Scale Tests to Eestimate the Failure Ddiameter of a Propellant*, Proceedings of the 9th International Detonation Symposium, Office of the Chief of Naval Research, OCNR 113291-1, pp.701-710.

Whelan, D.J. and Bocksteiner, G. (1998) *PBXW-115, an Extremely Insensitive Detonating Substance?* DSTO-TR-0632, AR-010-469, DSTO Technical Report, Melbourne, March.

Wilkinson, C. (2001) *A comparative study of the performance of the underwater IM explosive PBXW-115(AUST)*, DSTO-TR-1183, DSTO Technical Report, Melbourne, August 2001, distributed on CD-ROM.

Wood W.W. and Kirkwood J.G. (1954). Journal of Chemical Physics, **22** pp. 1920-1924.

DISTRIBUTION LIST

Modelling of PBXW-115 Using Kinetic CHEETAH and the DYNA Codes

Jing Ping Lu and David L. Kennedy

AUSTRALIA

DEFENCE ORGANISATION

	No. of copies
S&T Program	
Chief Defence Scientist	shared copy
FAS Science Policy	
AS Science Corporate Management	
Director General Science Policy Development	
Counsellor Defence Science, London	Doc Data Sheet
Counsellor Defence Science, Washington	Doc Data Sheet
Scientific Adviser Joint	1
Navy Scientific Adviser	Doc Data Sht & Dist List
Scientific Adviser - Army	Doc Data Sht & Dist List
Air Force Scientific Adviser	Doc Data Sht & Dist List
Scientific Adviser to the DMO M&A	Doc Data Sht & Dist List
Scientific Adviser to the DMO ELL	Doc Data Sht & Dist List
Director of Trials	1
Systems Sciences Laboratory	
Chief of Weapons Systems Division	Doc Data Sht & Dist List
Research Leader: Dr. N. Burman	Doc Data Sht & Dist List
Research Leader: Dr. N. Martin	Doc Data Sht & Dist List
Task Manager: Dr. W.S. Wilson	1
Author: Dr. J.P. Lu	3
Head of Weapons Propulsion Group	1
Head of Terminal Effects Group	1
Dr K. Krishnamoorthy	1
Dr P. Davis	1
Dr I. J. Lochert	1
Dr A. Provatas	1
Ms. Danielle Gilboy	1
Mr B. L. Hamshere	1
Mr M. W. Smith	1
Mr M. Franson	1
Dr F. Christo	1
Dr. A. White	1
Dr C. Doolan	1
Dr D. Jones, MPD	1
DSTO Library and Archives	
Library Edinburgh	1 & Doc Data Sheet
Australian Archives	1

Capability Systems Division
Director General Maritime Development — Doc Data Sheet
Director General Aerospace Development — Doc Data Sheet
Director General Information Capability Development — Doc Data Sheet

Office of the Chief Information Officer
Deputy CIO — Doc Data Sheet
Director General Information Policy and Plans — Doc Data Sheet
AS Information Structures and Futures — Doc Data Sheet
AS Information Architecture and Management — Doc Data Sheet
Director General Australian Defence Simulation Office — Doc Data Sheet

Strategy Group
Director General Military Strategy — Doc Data Sheet
Director General Preparedness — Doc Data Sheet

HQAST
SO (Science) (ASJIC) — Doc Data Sheet

Navy
Director General Navy Capability, Performance and Plans, Navy Headquarters — Doc Data Sheet
Director General Navy Strategic Policy and Futures, Navy Headquarters — Doc Data Sheet

Army
ABCA National Standardisation Officer, Land Warfare Development Sector, Puckapunyal — e-mailed Doc Data Sheet
SO (Science), Deployable Joint Force Headquarters (DJFHQ) (L), Enoggera QLD — Doc Data Sheet
SO (Science) - Land Headquarters (LHQ), Victoria Barracks NSW — Doc Data & Exec Summ

Intelligence Program
DGSTA Defence Intelligence Organisation — 1
Manager, Information Centre, Defence Intelligence Organisation — 1
Assistant Secretary Corporate, Defence Imagery and Geospatial Organisation — Doc Data Sheet

Defence Materiel Organisation
JALO, Defence Establishment Orchard Hills, NSW 2748
Attn: Head, Specialist Group — 1
Director Ordinance Safety Group
CP2-3-21 Campbell Park Offices
Canberra, ACT 2600 — 1
Head Airborne Surveillance and Control — Doc Data Sheet
Head Aerospace Systems Division — Doc Data Sheet
Head Electronic Systems Division — Doc Data Sheet
Head Maritime Systems Division — Doc Data Sheet
Head Land Systems Division — Doc Data Sheet

Defence Libraries

Library Manager, DLS-Canberra	Doc Data Sheet
Library Manager, DLS - Sydney West	Doc Data Sheet

OTHER ORGANISATIONS

National Library of Australia	1
NASA (Canberra)	1
Orica Explosives, George Booth Drive, PO Box 196, Kurri Kurri, NSW Attn: Dr. David L. Kennedy	1

UNIVERSITIES AND COLLEGES

Australian Defence Force Academy	
Library	1
Head of Aerospace and Mechanical Engineering	1
Serials Section (M list), Deakin University Library, Geelong, VIC	1
Hargrave Library, Monash University	Doc Data Sheet
Librarian, Flinders University	1

OUTSIDE AUSTRALIA

INTERNATIONAL DEFENCE INFORMATION CENTRES

US Defense Technical Information Center	2
UK Defence Research Information Centre	2
Canada Defence Scientific Information Service	1
NZ Defence Information Centre	1

ABSTRACTING AND INFORMATION ORGANISATIONS

Library, Chemical Abstracts Reference Service	1
Engineering Societies Library, US	1
Materials Information, Cambridge Scientific Abstracts, US	1
Documents Librarian, The Center for Research Libraries, US	1

INFORMATION EXCHANGE AGREEMENT PARTNERS

Acquisitions Unit, Science Reference and Information Service, UK	1
Library – Exchange Desk, National Institute of Standards and Technology, US	1
NMIC, NATO Headquarters, 110 Bruxelles, Belgium	1

SPARES	5
Total number of copies:	**52**

DEFENCE SCIENCE AND TECHNOLOGY ORGANISATION
DOCUMENT CONTROL DATA

1. PRIVACY MARKING/CAVEAT (OF DOCUMENT)

2. TITLE Modelling of PBXW-115 Using Kinetic CHEETAH and the DYNA Codes	3. SECURITY CLASSIFICATION (FOR UNCLASSIFIED REPORTS THAT ARE LIMITED RELEASE USE (L) NEXT TO DOCUMENT CLASSIFICATION) Document (U) Title (U) Abstract (U)
4. AUTHOR(S) Jing Ping Lu and David L. Kennedy	5. CORPORATE AUTHOR Systems Sciences Laboratory PO Box 1500 Edinburgh South Australia 5111 Australia

6a. DSTO NUMBER	6b. AR NUMBER	6c. TYPE OF REPORT	7. DOCUMENT DATE
DSTO-TR-1496	AR-012-899	Technical Report	September 2003

8. FILE NUMBER	9. TASK NUMBER	10. TASK SPONSOR	11. NO. OF PAGES	12. NO. OF REFERENCES
E9505-25-16	DST 01/138	DSTO	34	48

13. URL on the World Wide Web	14. RELEASE AUTHORITY
http://www.dsto.defence.gov.au/corporate/reports/DSTO-TR-1496.pdf	Chief, Weapons Systems Division

15. SECONDARY RELEASE STATEMENT OF THIS DOCUMENT

Approved for public release

OVERSEAS ENQUIRIES OUTSIDE STATED LIMITATIONS SHOULD BE REFERRED THROUGH DOCUMENT EXCHANGE, PO BOX 1500, EDINBURGH, SA 5111

16. DELIBERATE ANNOUNCEMENT

No Limitations

17. CITATION IN OTHER DOCUMENTS Yes

18. DEFTEST DESCRIPTORS

Plastic bonded explosives, Modelling

19. ABSTRACT

PBXW-115, a highly non-ideal explosive tailored for underwater effects and composed of 43% ammonium perchlorate, 25 % aluminium, 20% RDX and 12% HTPB binder, has been studied using Kinetic CHEETAH (the Lawrence Livermore National Laboratory CHEETAH 2.0 code), the three-term "Ignition and Growth" Model incorporated into the explicit finite element hydrocode LSTC-DYNA, and the CPeX Reactive Model based on the small divergent detonation theory of Wood and Kirkwood in DYNA2D. This report firstly focuses on a series of simulations performed using Kinetic CHEETAH based on the Wood-Kirkwood detonation theory using a pressure exponent of 2 in the pressure-dependent rate law. It was found that CHEETAH could predict the trend of the detonation velocity as a function of charge diameter, but overestimated the detonation velocities. The agreement was improved with further parameter adjustment, by decreasing the pressure exponent in the rate law from 2.0 to 1.0, and then 0.5. The reaction zone widths over a wide range of charge radius were also computed. Attention was then turned to hydrocode modelling, with particular interest in developing reactive models for PBXN-111 and PBXW-115 (*Aust*). Both the "Ignition and Growth" Model and the CPeX Model were calibrated against the experimentally observed dependence of detonation velocity on charge diameter in unconfined charges of both PBXW-115 (*Aust*) and US PBXN-111. These two reactive models were validated by comparing their predictions against experimental data for detonation of charges confined in 2.5 mm and 3 mm thick brass. The Ignition and Growth Model was then applied successfully to the simulation of aquarium tests. Finally, to test whether the two models using parameters derived from small-scale tests can be applied to large-scale devices, these two models were applied to the simulation of mid-scale underwater tests of PBXW-115 (*Aust*), and comparisons with available data are made. The LS-DYNA simulations of shock front curvature for unconfined charges are also presented and the relationships between the radii of curvature for the detonation fronts and self-propagating detonation velocities are discussed.